MASER AMPLIFICATION OF INCOHERENT RADIATION BY INTERSTELLAR OH*

A. Icsevgi and W. E. Lamb, Jr.
Yale University, New Haven, Connecticut

NGR-07-004-035

*Research sponsored by the Air Force Office of Scientific Research, Office of Aerospace Research, United States Air Force under AFOSR Grant No. 1324-67, and in part by the National Aeronautics and Space Administration.

ABSTRACT

A model is proposed for the maser amplification of the emission lines of interstellar OH. Weak incoherent microwave radiation from an external source passes through an OH cloud and is enhanced by maser action. The amplifying medium is considered as a collection of thermally moving two-level molecules which undergo excitation to the upper level at a steady pump rate. The details of the pumping mechanism as well as the state of polarization of the radiation are not considered. The natural linewidth and the spontaneous decay of the two levels are represented by phenomenological constants γ_{ab}, γ_a and γ_b. The Maxwell's equations for the electromagnetic field are coupled to the quantum mechanical equations of motion for the molecular density matrix in a self-consistent way. After reducing the equations on the basis of slowly varying amplitude and narrow passband approximations, a single equation is derived for the spectral density by assuming that the incoming radiation is completely incoherent. The steady-state solutions of this equation are investigated analytically and the equation itself is integrated numerically for several kinds of Doppler broadening. It is found that in the absence of molecular motion, the spectrum approaches a δ-function at the resonance frequency as the radiation travels through the medium. However when Doppler broadening is introduced, the behaviour of the spectral density is dependent upon the relative magnitude of the Doppler width with respect to the homogeneous linewidth and upon the amount by which threshold is exceeded.

I. INTRODUCTION

Since the discovery of the first microwave lines of the interstellar hydroxyl radical in October 1963, there have been extensive astronomical observations[1-7] of four radio lines at 1612, 1665, 1667 and 1720 MHz, arising from transitions between the hyperfine levels of the Λ doublet in the ground state of OH.

These lines have been observed in absorption, emission or both in the spectra of a large number of radio sources close to the galactic plane.[8] The emission from OH molecules is decidedly non-thermal. Besides extremely narrow spectral profiles, the salient characteristics of the observations include a very small angular size of the emitting region, a lower limit on the surface brightness of the order of 10^3K, strong polarization both linear and circular and finally intensity ratios for the four lines in disagreement with their theoretical values.

These properties suggest that the observed signals have been amplified by stimulated emission. At least in a qualitative way, maser amplification could indeed account for most of the anomalous features that have been observed. A peaked gain profile produces progressive narrowing of the spectrum as the signal travels through the medium. The details of the pumping mechanism may cause the populations of the levels to be different than what they would be in thermal equilibrium and thus lead to intensity ratios in disagreement with those predicted by theoretical line strengths. Further, as was shown by several authors,[9-11] stimulated emission may be polarized while thermal emission could not.

A variety of schemes have been invented[12-20] to describe the mechanism by which the OH cloud would be pumped up to excited levels as required for maser action to take place. The nature of the fluctuation that triggers maser amplification is also a matter for speculation. One possibility is the amplification of light spontaneously emitted within the medium. However, emission has been seen so far only against continuous sources and even if there were no nearby source of continuum to serve as input to the maser, the background microwave radiation from the Galaxy would be an effective stimulus.

For a more comprehensive presentation of the subject the reader is referred to review articles.[21,22]

The problem of coherent light, whether it be a monochromatic wave or a pulse, propagating through a maser amplifier has been widely investigated by numerous authors.[23-33] On the other hand, the propagation of incoherent radiation, such as white noise or black body radiation, does not follow in any direct way from these investigations because of the nonlinear aspects of the problem.

We propose in this paper to give a simple model which describes the amplification of an incoherent input signal by a two-level gaseous medium. It will be assumed that the population of the levels is inverted at a steady rate but the details of this pumping mechanism will be ignored. The paper is divided into six sections. In the next section we summarize the derivation of the equations for the propagation of a general electromagnetic field in a two-level medium. In Sec. III the equations are specialized to the case of fixed molecules (homogeneous broadening) and reduced on the basis of several approximations appropriate to our problem such as the slowly varying amplitude, the narrow passband and the third order perturbation approximations. In Sec. IV, the incoherent radiation is described in terms of its spectral properties and an equation is derived for the propagation of the spectral density function. After a brief study of this equation, the results are generalized to the case of a strong signal by summing the perturbation expansion series. Section V introduces the motion of the molecules (Doppler broadening). General conclusions are drawn in Sec. VI.

II. DERIVATION OF THE EQUATIONS

The basis for the following calculations was set by Lamb in his 'Theory of an Optical Maser'. The gas cloud will be assumed to be a collection of two-level molecules in thermal motion and coupled only through their dipole interaction with the overall field. The latter will be represented by a scalar $E(z,t)$ linearly polarized in the x-direction and propagating in the z direction.

$$\underset{\sim}{E}(\underset{\sim}{r},t) = E(z,t)\ \hat{x} \tag{1}$$

Thus the problem is reduced to a single dimension and no attempt is made to describe the actual polarization of the field arising from the magnetic splitting of the levels. Collision effects will also be ignored.

Given two time independent basis functions ψ_a, ψ_b for the states a and b, the wave function for the molecule can be written as

$$\psi(t) = a(t)\psi_a + b(t)\psi_b\ . \tag{2}$$

In the subspace spanned by ψ_a and ψ_b the effective Hamiltonian seen by the molecule is

$$H = H_o - E\wp \tag{3}$$

where

$$H_o = \hbar \begin{pmatrix} \omega_a & o \\ o & \omega_b \end{pmatrix} \tag{4}$$

is the Hamiltonian for the unperturbed molecule,

$$E\wp = \begin{pmatrix} o & pE(t) \\ pE(t) & o \end{pmatrix} \tag{5}$$

is the interaction Hamiltonian in the dipole approximation, and

$$p = \langle a|\wp|b\rangle = \langle b|\wp|a\rangle \tag{6}$$

is the matrix element of the dipole moment operator $\wp$. The density matrix $\rho(\alpha, z_o, t_o, v, t)$ of the molecule, labelled by the initial state $\alpha(\alpha{=}a$ or $b)$, position z_o, time t_o and velocity v of excitation is defined as

$$\rho = |\psi\rangle\langle\psi| \tag{7}$$

and is known to obey the equation of motion

$$i\hbar\, \partial\rho/\partial t = [H, \rho] \; . \tag{8}$$

The expectation value of the molecular dipole moment is given by

$$\langle\wp\rangle = \mathrm{Tr}(\rho\wp) = p(\rho_{ab} + \rho_{ba}) \; . \tag{9}$$

A proper statistical summation over (9) leads to the macroscopic polarization P(z,t) which enters as a driving term into Maxwell's equation for the field. Leaving the summation over v aside, for the time being, it can be seen that

$$\rho(v,z,t) = \sum_{\alpha=a}^{b} \int_{-\infty}^{t} dt_o \int dz_o \; \lambda_\alpha(v,z_o,t_o)\,\rho(\alpha,z_o,t_o,v;t)\,\delta(z-z_o-v(t-t_o)) \tag{10}$$

where λ_α is the number of atoms excited to state α per unit time and unit volume, represents the population matrix for an ensemble of molecules of a given velocity v which reach the position z at time t and thus contribute to the polarization according to

$$P(z,t) = \int dv\; P(v,z,t) = p\int dv\;[\rho_{ab}(v,z,t) + \rho_{ba}(v,z,t)]. \tag{11}$$

It has been shown elsewhere[33] that in terms of $\rho(v,z,t)$, the coupling of the equation of motion (8) to the field equation, can be written as

$$-\partial^2E/\partial z^2 + \mu_o\sigma\partial E/\partial t + c^{-2}\partial^2E/\partial t^2 = -\mu_o\partial^2P(z,t)/\partial t^2 \tag{12a}$$

$$(\partial/\partial t + v\partial/\partial z)\,\rho_{aa}(v,z,t) = \lambda_a - \gamma_a\rho_{aa} - i(p/\hbar)E(z,t)\;(\rho_{ab}-\rho_{ba}) \tag{12b}$$

$$(\partial/\partial t + v\partial/\partial z)\,\rho_{bb}(v,z,t) = \lambda_b - \gamma_b\rho_{bb} + i(p/\hbar)E(z,t)\;(\rho_{ab}-\rho_{ba}) \tag{12c}$$

$$(\partial/\partial t + v\partial/\partial z)\,\rho_{ab}(v,z,t) = -(\gamma_{ab} + i\omega)\,\rho_{ab} - i(p/\hbar)E(z,t)(\rho_{aa}-\rho_{bb}) \tag{12d}$$

$$\rho_{ba}(v,z,t) = \rho_{ab}^{*} \;, \tag{12e}$$

where μ_o is the vacuum permeability, c the velocity of light and ω the resonance frequency

$$\omega = \omega_a - \omega_b \;. \tag{13}$$

The fictitious conductivity σ is introduced phenomenologically in order to account for any linear losses in the background medium. The damping constants γ_a, γ_b and γ_{ab} are similarly introduced to represent the decay of the levels a, b and of the molecular dipole moment in the absence of any radiation field. Further, a steady and homogeneous rate of excitation is assumed, so that

$$\lambda_\alpha (v,z,t) = \Lambda_\alpha W(v) \tag{14}$$

where W(v) is the velocity distribution function.

Given initial conditions $\rho(v,z,0)$ for the medium and the boundary condition $E(0,t)$ for the field, Eqs. (12) in principle determine $E(z,t)$ for any z. However, the integration of the equations is not practically feasible and further approximations must be used. The nature of these approximations depends on the form of the input signal. In the following section we shall specialize Eqs. (12) for the case of incoherent input.

To exhibit more clearly the novel features of the problem we shall first treat the case of fixed molecules leaving aside the interesting but otherwise familiar complication of molecular motion. In this case the medium is said to be homogeneously broadened.

III. SIMPLIFYING APPROXIMATIONS

1. Fixed Molecules (Homogeneous Broadening).

Setting v = 0 and dropping any velocity dependence of the variables, we may reduce Eqs. (12) to

$$-\partial^2 E/\partial z^2 + \mu_o \sigma \partial E/\partial t + c^{-2}\partial^2 E/\partial t^2 = -\mu_o \partial^2 P/\partial t^2 \tag{15a}$$

$$\dot{\rho}_{aa} = \lambda_a - \gamma_a \rho_{aa} - i(p/\hbar)\, E(\rho_{ab} - \rho_{ba}) \tag{15b}$$

$$\dot{\rho}_{bb} = \lambda_b - \gamma_b \rho_{bb} - i(p/\hbar)\, E(\rho_{ab} - \rho_{ba}) \tag{15c}$$

$$\dot{\rho}_{ab} = -(\gamma_{ab} + i\omega)\, \rho_{ab} - i(p/\hbar) E(\rho_{aa} - \rho_{bb}) \tag{15d}$$

$$\rho_{ba} = \rho_{ab}^* \ . \tag{15e}$$

Since an incoherent field is much more easily described in terms of its spectral properties, it will clearly be helpful to work in the frequency domain. Introducing the Fourier transforms

$$E(z,\nu) = (2\pi)^{-1} \int_{-\infty}^{+\infty} E(z,t) e^{-i\nu t}\, dt \quad , \tag{16a}$$

$$\rho(z,\nu) = (2\pi)^{-1} \int_{-\infty}^{+\infty} \rho(z,t) e^{-i\nu t}\, dt \tag{16b}$$

and assuming $\gamma_{ab} \ll \omega$, Eqs. (15) are transformed into

$$\partial^2 E(z,\nu)/\partial z^2 = -(\nu^2/c^2 - i\nu\mu_o\sigma) E(z,\nu) - \mu_o \nu^2 P(z,\nu) \tag{17a}$$

$$P(z,\nu) = (p^2/\hbar)\left[2\omega/(\nu^2 - \omega^2 - 2i\gamma_{ab}\nu)\right] \int_{-\infty}^{+\infty} N(z,\nu') E(z,\nu-\nu') d\nu' \tag{17b}$$

$$N(z,\nu) = N_o\delta(\nu) + (\hbar\omega)^{-1}\left[(\gamma_a + i\nu)^{-1} + (\gamma_b + i\nu)^{-1}\right]$$
$$\times \int_{-\infty}^{+\infty} i\nu' P(z,\nu')\, E(z,\nu-\nu')\, d\nu' \qquad (17c)$$

where

$$P(z,\nu) = p[\rho_{ab}(z,\nu) + \rho_{ba}(z,\nu)] \,, \qquad (18)$$

$$N(z,\nu) = \rho_{aa}(z,\nu) - \rho_{bb}(z,\nu) \qquad (19)$$

and

$$N_o = (\Lambda_a/\gamma_a) - (\Lambda_b/\gamma_b) \qquad (20)$$

is the population inversion that would be established in the absence of any field.

2. Slowly Varying Amplitude Approximation

Equation (17-a) suggests that $E(z,\nu)$ has a rapidly varying dependence $\exp(-i\nu z/c)$. In order to remove this factor we set

$$E(z,\nu) \rightarrow E(z,\nu)\exp(-i\nu z/c) \qquad (21a)$$

$$P(z,\nu) \rightarrow P(z,\nu)\exp(-i\nu z/c) \qquad (21b)$$

$$N(z,\nu) \rightarrow N(z,\nu)\exp(-i\nu z/c) \,. \qquad (21c)$$

Equations (17b) and (17c) are not affected by these substitutions.

However, assuming that the new $E(z,\nu)$ varies slowly over a distance c/ν, Eq. (17a) reduces to a first order equation

$$\partial E/\partial z = -\frac{1}{2}\mu_o\sigma c E - \frac{1}{2} i\mu_o \nu c P \quad . \tag{22}$$

3. Scaling of the Equations

Equations (17b), (17c) and (21) are reduced to a convenient form if E, P, N are evaluated in units of E_o, P_o, N_o respectively, with

$$E_o = (\hbar/p)\ (\gamma\gamma_{ab})^{1/2} \quad , \tag{23a}$$

$$P_o = ipN_o\ (\gamma/\gamma_{ab})^{1/2} \quad , \tag{23b}$$

$$\gamma = 2(\gamma_a^{-1} + \gamma_b^{-1})^{-1} \tag{23c}$$

and N_o is given by (20). In these units the resulting equations can be written as

$$\partial E(z,\nu)/\partial z = -\varkappa E(z,\nu) + \mathcal{G} P(z,\nu) \tag{24a}$$

$$P(z,\nu) = 2i\gamma_{ab}\omega[\omega^2 - \nu^2 + 2i\gamma_{ab}\nu]^{-1}\int_{-\infty}^{+\infty} N(z,\nu')E(z,\nu-\nu')d\nu' \tag{24b}$$

$$N(z,\nu) = \delta(\nu) - F(\nu)\int_{-\infty}^{+\infty} (\nu'/\omega)\ P(z,\nu')E(z,\nu-\nu')d\nu' \tag{24c}$$

where the linear loss $\varkappa$ and the coupling constant $\mathcal{G}$ are given by

$$\varkappa = \frac{1}{2}\mu_o\sigma c \tag{25}$$

and

$$\mathcal{G} = \frac{1}{2} p^2 N_o/(\epsilon_o \hbar\gamma_{ab} c) \quad . \tag{26}$$

The function $F(\nu)$ is defined as

$$F(\nu) = \gamma[(\gamma_a + i\nu)^{-1} + (\gamma_b + i\nu)^{-1}] \quad . \qquad (27)$$

The new variables E, P, N which enter Eqs. (24) have the dimension of a frequency and represent the Fourier transforms of dimensionless quantities, while $\varkappa$ and $\mathcal{G}$ have the dimensions of a reciprocal length.

4. Narrow Passband Approximation

Since the natural bandwidth of the amplifier, of the order of γ_{ab}, is much smaller than the resonance frequency ω, $E(z,\nu)$ and $P(z,\nu)$ will have appreciable values only around a limited range of frequencies around $\nu = \pm\,\omega$. Similarly $N(z,\nu)$ will be peaked around $\nu = 0$. It is therefore expedient to modify the integrals appearing in Eqs. (24), using these properties of the integrands.

The factor in front of the integral in (24b) can be reduced to a complex Lorentzian if we set

$$\nu = \omega + \Omega \qquad (28)$$

where Ω is small compared to ω. We then find

$$2i\gamma_{ab}\omega(\omega^2 - \nu^2 + 2i\gamma_{ab}\nu)^{-1} \simeq \gamma_{ab}/(\gamma_{ab} - i\Omega) = D(\Omega) \quad . \qquad (29)$$

The main contribution to the integral in Eq. (24b) comes from small values of ν', so that in terms of the translated functions

$$P(z,\ \omega + \Omega) \rightarrow P(z,\Omega) \tag{30a}$$

$$E(z,\omega + \Omega - \Omega') \rightarrow E(z,\Omega - \Omega') \tag{30b}$$

Eq. (24b) may be approximated by

$$P(z,\Omega) = D(\Omega) \int N(z,\Omega') \ E(z,\Omega-\Omega') \ d\Omega' \ , \tag{31}$$

where the dummy variable ν' has been replaced by Ω'.
Appreciable contributions to the integral in (24c) come from two regions: the first is $\nu' \sim \omega$, the second $\nu' \sim -\omega$. Changing the variable of integration to Ω' defined by

$$\nu' = \omega + \Omega' \tag{32}$$

in the first region, and by

$$\nu' = -\omega + \Omega-\Omega' \tag{33}$$

in the second region, Eq. (24c) may be expressed in terms of the translated functions of (30), as

$$N(z,\Omega) = \delta(\Omega) - F(\Omega)\int[P(z,\Omega')E^{*}(z,\Omega'-\Omega) + E(z,\Omega')P^{*}(z,\Omega'-\Omega)]d\Omega' \tag{34}$$

where use was made of the symmetry property

$$E(z,\ -\nu) = E^{*}(z,\nu) \text{ and } P(z,\ -\nu) = P^{*}(z,\nu) \tag{35}$$

and of the approximations

$$\Omega,\Omega' << \omega \ . \tag{36}$$

The complete set of coupled equations is then

$$\partial E/\partial z = -\kappa E + \mathcal{G}P \tag{37a}$$

$$P = \mathcal{D}(\Omega)\int N(z,\Omega')E(z,\Omega-\Omega')d\Omega' \tag{37b}$$

$$N = \delta(\Omega)-F(\Omega)\int[P(z,\Omega')E^*(z,\Omega'-\Omega) + E(z,\Omega')P^*(z,\Omega'-\Omega)]d\Omega' \tag{37c}$$

5. Third Order Iteration

An iterative solution of the form

$$N(z,\Omega) = N^{(0)} + N^{(2)} + N^{(4)} + \ldots \tag{38a}$$

$$P(z,\Omega) = P^{(1)} + P^{(3)} + P^{(5)} + \ldots \tag{38b}$$

can be written down for the coupled integral equations (37b) and (37c). Under certain conditions, to be specified later, the truncated form of (38) represents an adequate approximation to the true solution. Using

$$N^{(0)} = \delta(\Omega) \tag{39}$$

one obtains by repeated substitutions

$$P^{(1)} = D(\Omega)E(\Omega) , \tag{40}$$

$$N^{(2)} = -F(\Omega)\int d\Omega' E(\Omega')E^*(\Omega'-\Omega)[D(\Omega') + D^*(\Omega'-\Omega)] \tag{41}$$

and

$$P^{(3)} = -D(\Omega)\int d\Omega' E(\Omega-\Omega')F(\Omega')\int d\Omega'' E(\Omega'')E^*(\Omega''-\Omega')[D(\Omega'') + D^*(\Omega''-\Omega')] \tag{42}$$

Hence the third order field equation

$$\partial E/\partial z = [\mathcal{G}D(\Omega)-\varkappa]E-\mathcal{G}D(\Omega)\int d\Omega' E(\Omega-\Omega')F(\Omega')\int d\Omega'' E(\Omega'')E^*(\Omega''-\Omega')[D(\Omega'')+D^*(\Omega''-\Omega' \tag{43}$$

6. Numerical Integration

We have attempted to integrate Eq. (43) numerically with a digital computer. In order to perform such an integration one must choose a set of discrete frequencies Ω_n for which one wishes to determine the z dependence of $E(z,\Omega_n)$. The distribution of the Ω_n's along the Ω axis must be dense enough inside the passband so that one may evaluate accurately the integrals on the right hand side of (43). However, the number of operations involved in evaluating these integrals increases roughly as the square of the number N of frequencies used and is of the order of 4000 multiplications and 7000 additions for N = 20. This rapidly produces an accumulation of round-off errors such that the accurate integration of the equation becomes very costly. There is also a more fundamental objection to the direct numerical integration of Eq. (43). Assuming that a discrete set of representative frequencies Ω_n has been chosen, one would then like to assign random phases to the boundary values $E(0,\Omega_n)$ to express the erratic behavior of the Ω dependence of the phase of $E(0,\Omega)$. It is then illegitimate to replace integrals over such a rapidly varying function by a sum over a few discrete frequencies. Somehow, use must be made of the randomness of the phases in evaluating these integrals.

However, Eq. (43) is not entirely useless. If one claims that the incoming signal contains only a few discrete frequencies, then the right hand side reduces to a manageable sum, and one could integrate the equation at reasonable cost. Care must be taken to choose the discrete frequencies in such a way that by forming combination tones one does not obtain new frequencies falling inside the passband. This is most simply achieved by covering the passband with equally spaced frequencies.

We have carried out this calculation with up to 9 frequencies, repeating each case several times with different choices of the initial random phases. The result was invariably a disappearance of the sidebands and a building up of the central frequency to the value predicted by the single frequency theory[33] (see Fig. 1). Examination of Eq. (43) shows that this, as well as oscillation at any other single frequency, is a stable solution. An obvious reason for the building up of the central frequency at the expense of the sidebands is the favorable gain conditions. If the sidebands were more numerous and closely spaced, it is conceivable that the random choice of the initial phases might favor some sideband not far from the center, in spite of its relatively lower gain. However, with only 9 frequencies covering the entire passband, even the first sidebands have a gain so much lower that the combinations of initial phases required to produce a build-up of anything but the center frequency is extremely unlikely and never occurred in the limited number of trials we made.

IV. INCOHERENT RADIATION

1. Description of the Radiation Field

We shall now specify the nature of the radiation field $E(0,t)$ hitting the entry plane $z = 0$. A qualitative picture of incoherent light is a superposition of many frequencies with uncorrelated phases and possibly fluctuating intensities. If the complex amplitude $E(0,\Omega)$ of the Fourier transform of $E(0,t)$ is written in polar form as

$$E(0,\Omega) = A(\Omega)\exp[i\theta(\Omega)] \quad , \tag{44}$$

$A^2(\Omega)$ gives the intensity and $\theta(\Omega)$ the phase of the particular frequency Ω. We would therefore assume that $A^2(\Omega)$ is fluctuating around an average value $I(\Omega)$ which itself may vary smoothly with Ω and that $\theta(\Omega)$ is an erratic function of Ω whose values are distributed with a uniform probability density between 0 and 2π. (By an erratic function we mean that any sequence of values of the function passes the randomness tests.)

The incoherent character of the field implies that the phases of two distinct frequencies, no matter how close, are totally uncorrelated. In practice of course, there will be a very small frequency ν_c called the coherence range such that frequencies within the same coherence range do have correlated phases, however, ν_c will be assumed to be much smaller than all other frequencies relevant to the problem.

The Fourier transform of a signal with a discrete set of frequencies can be written as

$$E(\Omega) = \sum_n E_n \delta(\Omega - n\,\delta\Omega) \qquad (45)$$

where $\delta\Omega$ is the spacing of the allowed frequencies. (Note that the complex amplitudes E_n are dimensionless.) The total energy is proportional to

$$W = \sum_n |E_n|^2 \quad . \qquad (46)$$

The assumption of no correlation can be expressed by the following condition on the E_n's

$$\lim_{\delta\Omega/\Delta\Omega \to 0} (\Delta\Omega)^{-1} \sum_{n \epsilon \Delta\Omega} E_n E^*_{n+n'} = \delta_{n',0} I(\Omega) \qquad (47)$$

where $\Delta\Omega$ is a frequency interval around Ω, small compared to the bandwidth of the medium, but large compared to $\delta\Omega$. The notation $n \epsilon \Delta\Omega$ means that $n\delta\Omega$ falls inside the interval $\Delta\Omega$ (see Fig. 2). The limit in (47) must be understood in the probabilistic sense. In more precise terms, given any $\epsilon > 0$ and $0 < P_0 < 1$, we can choose N so large that the probability of having

$$(\Delta\Omega)^{-1} \sum_{n \epsilon \Delta\Omega} E_n E^*_{n+n'} < \epsilon \qquad (n' \neq 0) \qquad (48)$$

is larger than p_0.

When $n' = 0$, Eq. (47) becomes the defining relation for the function $I(\Omega)$ which can be recognized as the spectral density since we have, from (46) and (47)

$$W = \sum_{\Delta\Omega} I(\Omega)\Delta\Omega = \int_{-\infty}^{+\infty} I(\Omega)d\Omega \quad . \tag{49}$$

2. Derivation of the Reduced Equation

For a discrete spectrum like that of (45), Eq. (43) becomes

$$\partial E_n/\partial z = (GD_n - \varkappa)E_n - GD_n \sum_{n'} E_{n-n'}F_{n'} \sum_{n''} E_{n''}E^*_{n''-n'}(D_{n''} + D^*_{n''-n'}) \tag{50}$$

where

$$D_n = D(n\delta\Omega) \text{ and } F_{n'} = F(n'\delta\Omega) \ . \tag{51}$$

Subdividing the Ω axis into small intervals $\Delta\Omega$ over which $D(\Omega)$ and $F(\Omega)$ remain practically constant, we have

$$\partial E_n/\partial z = (GD_n - \varkappa)E_n - GD_n \sum_{n'} E_{n-n'}F_{n'} \sum_{\Delta\Omega''} [D(\Omega'') + D^*(\Omega''-\Omega')]$$

$$\times \sum_{n''\epsilon\Delta\Omega''} E_{n''}E^*_{n''-n'} \tag{52}$$

Now, if $N = \Delta\Omega/\delta\Omega$ is a very large number, we can use (47) to transform (52) into

$$\partial E_n/\partial z = (GD_n - \varkappa)E_n - 4GD_nE_n \sum_{\Delta\Omega''} L(\Omega'')\, I(\Omega'')\Delta\Omega'' \tag{53}$$

where we used

$$F_0 = F(0) = 2 \tag{54}$$

and

$$L(\Omega) = \tfrac{1}{2}[D(\Omega) + D^{*}(\Omega)] = \gamma_{ab}^{2}/(\gamma_{ab}^{2} + \Omega^{2}) \ . \qquad (55)$$

Applying the operator $(\Delta\Omega)^{-1} \sum_{n\epsilon\Delta\Omega} E_n^{*}$ to both sides of Eq. (53), we find

$$\partial I/\partial z = 2[\mathcal{G}L(\Omega)-\varkappa]I(\Omega) - 8\mathcal{G}L(\Omega)I(\Omega)\int L(\Omega')I(\Omega')d\Omega' \qquad (56)$$

where the discrete sum of (53) has now been replaced by an integral. To summarize the situation, we have transformed Eq. (43) involving amplitudes and phases, into Eq. (56) involving the spectral density $I(z,\Omega)$ by assuming that the radiation hitting the entry plane $z = 0$ is incoherent as expressed by the condition (47).

Since we don't yet know whether the radiation field remains incoherent as it travels through the active medium, we can only claim that Eq. (56) holds at $z = 0$. We will now show that the field at some small depth Δz is also incoherent. Defining

$$M(z) = 1-4\int L(\Omega')I(z,\Omega')d\Omega' \qquad (57)$$

we can write (53) as

$$[\partial E_n/\partial z]_{z=0} = [\mathcal{G}D_n M(0)-\varkappa]E_n(0) \qquad (58)$$

and we use it to calculate

$$(\partial/\partial z)[(\Delta\Omega)^{-1} \sum_{n\epsilon\Delta\Omega} E_n E_{n+n'}^{*}]_{z=0} = (\Delta\Omega)^{-1} \sum_{n\epsilon\Delta\Omega} [E_{n+n'}^{*}(z)\partial E_n(z)/\partial z + E_n(z)\partial E_{n+n'}^{*}(z)/\partial z]_{z=0} \qquad (59)$$

The first term on the right hand side becomes

$$(\Delta\Omega)^{-1} \sum_{n\epsilon\Delta\Omega} [\mathcal{G}D_n M(0)-\varkappa]E_n(0)E_{n+n'}^{*}(0) = [\mathcal{G}D(\Omega)M(0)-\varkappa]\delta_{n,0}I(0,\Omega), \qquad (60)$$

and the second term is given by a similar expression, so that

$$(\partial/\partial z)[(\Delta\Omega)^{-1}\sum_{n\epsilon\Delta\Omega} E_n(z)E^*_{n+n'}(z)]_{z=0} = 2[\mathcal{G}L(\Omega)M(0)-\kappa]\delta_{n',0}I(0,\Omega). \quad (61)$$

Hence

$$(\Delta\Omega)^{-1}\sum_{n\epsilon\Delta\Omega} E_n(\Delta z)E^*_{n+n'}(\Delta z) = \delta_{n',0}\{I(0,\Omega)+2\Delta z[\mathcal{G}L(\Omega)M(0)-\kappa]I(0,\Omega)\}$$

$$= \delta_{n',0}I(\Delta z,\Omega) \quad . \quad (62)$$

We have thus proved that the field obeys the condition (47) for incoherence at some small depth Δz and we may, by induction, extend the result to any depth z. Therefore Eq. (56) holds at any point of the medium and is written as

$$\partial I(z,\Omega)/\partial z = [L(\Omega)-\kappa]I(z,\Omega)-4L(\Omega)I(\Omega)\int L(\Omega')I(\Omega')d\Omega' \quad (63)$$

after expressing z and κ in units of $(2\mathcal{G})^{-1}$ and $\mathcal{G}$, respectively

$$2\mathcal{G}z \rightarrow z \quad , \quad \kappa/\mathcal{G} \rightarrow \kappa \quad . \quad (64)$$

We have gone through considerable detail to show how under the assumption of incoherent radiation, Eq. (43) becomes Eq. (53) which in turn gives Eq. (63). It can be noticed, however, that the same result is obtained by formally replacing the inner integral in (43) by

$$\int d\Omega''E(\Omega'')E^*(\Omega''-\Omega')[D(\Omega'')+D^*(\Omega''-\Omega')] \rightarrow \delta(\Omega')\int d\Omega''I(\Omega'')[D(\Omega'')+D^*(\Omega'')] \quad (65)$$

In future derivations this shortcut will be used rather than going through the same exact derivation over and over again.

The physical meaning of Eq. (63) is very simple. The increment in the spectral density is the difference of two terms. The first term is a net linear gain or loss with a Lorentzian profile

$$G(\Omega) = L(\Omega) - \varkappa \tag{66}$$

shown in Fig. 3, and from which it is clear that only those frequencies around $\Omega = 0$ ($\nu = \omega$) such that $G(\Omega) > 0$ will be amplified. In the absence of the nonlinear term, the linear gain would produce an exponential growth of all frequency components within the passband and an increasing sharpness of the spectral profile. It is seen from the second term that the saturation factor

$$S(z) = 4\int L(\Omega')I(z,\Omega')d\Omega' \tag{67}$$

is a weighted sum of contributions from all frequencies. Expressed in different terms this means that the various frequency components of the field act on the medium independently and then in turn each frequency component sees the overall saturation. This simple type of interaction is of course a direct consequence of dealing with an incoherent field. There is here an analogy with interference experiments in which two beams of light are superimposed. When the beams are coherent, the electric field amplitudes add up, while one only gets an addition of the intensities if the beams are incoherent.

3. Investigation of the Solutions

We shall now proceed to investigate the solutions of Eq. (63). We may first notice that this equation contains the possibility of oscillation at any single frequency within the gain bandwidth. Setting

$$I(z,\Omega) = A(z)\delta(\Omega-\Omega_o) \tag{68}$$

and substituting into (63) we get

$$dA/dz = [L(\Omega_o)-\kappa]A(z) - 4[L(\Omega_o)A(z)]^2 \tag{69}$$

which is similar to an equation obtained in our previous work.[33] Equation (69) gives a limiting value for A(z)

$$A(\infty) = [L(\Omega_o)-\kappa]/[2L(\Omega_o)]^2. \tag{70}$$

This approach may be generalized by writing, instead of (68) a sum of many δ-functions

$$I(z,\Omega) = \sum_j A_j(z)\delta(\Omega-\Omega_j) \; . \tag{71}$$

One would then obtain coupled equations for the various amplitudes A_i.

$$dA_i/dz = [L(\Omega_i)-\kappa]A_i(z) - 4L(\Omega_i)A_i(z) \sum_j L(\Omega_j)A_j(z) \tag{72}$$

which imply that if $A_k(z)$ is zero initially, it remains zero. Thus the generation of combination tones is now excluded from the theory. One should not be surprised by this result since the derivation of Eq. (63) was based on the assumption that between any two discrete frequencies such as Ω_k and Ω_{k+1} there actually is a very large number of intermediate frequencies with uncorrelated phases. The equation should therefore only be applied to a quasi-continuum of frequencies.

To investigate the possibility of a stationary solution by which we mean

$$I(z,\Omega) = I(\Omega) \tag{73}$$

we set the left-hand side of (63) equal to zero and obtain

$$\int L(\Omega')I(\Omega')d\Omega' = [L(\Omega)-\varkappa]/4L(\Omega) \tag{74}$$

after cancellation by $I(\Omega)$. Since this relation cannot be satisfied for all values of Ω, it appears that stationary solutions are not in general possible. Indeed the numerical integration of (63) starting with

$$I(0,\Omega) = \text{small constant} \tag{75}$$

shows (see Fig. 4) that the solution becomes increasingly peaked at $\Omega = 0$ thus asymptotically approaching the solution (68) for $\Omega_o = 0$, with

$$A(\infty) = (1-\varkappa)/4 \tag{76}$$

in agreement with (70). Loosely speaking we will say that $\delta(\Omega)$ is a stationary solution for Eq. (63), meaning that there is an actual solution $I(z,\Omega)$ such that

$$\lim_{z\to\infty} I(z,\Omega) = \delta(\Omega) . \tag{77}$$

It can be noticed that a sum of more than one δ-functions cannot be a stationary solution since setting the left hand sides equal to zero in Eqs. (72) results in a set of mutually inconsistent equations for the amplitudes A_i.

In the exceptional case $\varkappa = 0$, the solution does settle down to a stationary form just as soon as (74) is satisfied. However, it will be seen later that this is only an unphysical peculiarity of the third order equation.

4. Strong Signal Theory

The basic Eqs. (37) were decoupled using an iterative approach and truncating at third order on the assumption of a weak signal. It is in principle possible to write down the iterative solution to any order but the terms of higher order become increasingly complicated and the summation of the series does not seem to be feasible. However, we will be able to carry out this summation in our problem by using the simplifications brought about by the assumption of incoherence.

Starting again with the expansion (38) we successively obtain from (37)

$$N^{(o)} = \delta(\Omega) \tag{78}$$

$$P^{(1)} = D(\Omega)E(z,\Omega) \tag{79}$$

$$N^{(2)} = -F(\Omega)\int d' E(z,\Omega')E^*(z,\Omega'-\Omega)[D(\Omega') + D^*(\Omega'-\Omega)] \ . \tag{80}$$

Using the recipe of (65) we know that for an incoherent E, the last expression reduces to

$$N^{(2)} = -4\delta(\Omega)\int d\Omega' I(z,\Omega')L(\Omega') \equiv -S(z)\delta(\Omega) \ . \tag{81}$$

We may then proceed to find

$$P^{(3)} = -S(z)D(\Omega)E(z,\Omega) \ . \tag{82}$$

In order to derive the general formula for $P^{(2m+1)}$ by induction, we assume

$$P^{(2m+1)} = (-S)^m D(\Omega)E(\Omega) \quad , \tag{83}$$

where the z dependence of S and E is understood.
Substitution into (37c) gives

$$N^{(2m+2)} = -(S)^m \, F(\Omega)\int d\Omega' E(\Omega')E^*(\Omega'-\Omega)[D(\Omega') + D^*(\Omega'-\Omega)] \tag{84}$$

$$= (-S)^{m+1}\delta(\Omega) \quad ,$$

hence

$$P^{(2m+3)} = (-S)^{m+1}D(\Omega)E(\Omega)$$

which proves formula (83). We may now sum the series expansion

$$P = \sum_{m=o}^{\infty} P^{(2m+1)} = D(\Omega)E(\Omega)\sum_{m=o}(-S)^m = D(\Omega)E(\Omega)(1+S)^{-1} \tag{86}$$

and write Eq. (37a) as

$$\partial E/\partial z = -\varkappa E + G D(\Omega)E(\Omega)(1+S)^{-1} \tag{87}$$

which using (67) implies

$$\partial I(z,\Omega)/\partial z = \{-\varkappa + L(\Omega)/(1+4\int L(\Omega')I(z,\Omega')d\Omega')\}I(z,\Omega) \tag{88}$$

after using the scaling indicated in (64).
Equation (88) is the exact form of Eq. (63) and has much the same behaviour as the latter, namely its solutions approach $\delta(\Omega)$

as $z \to \infty$. According to (88) the limiting value of the expansion parameter is

$$S(\infty) = 4\int L(\Omega')I(\infty,\Omega')d\Omega' = \varkappa^{-1} - 1 , \tag{89}$$

The condition for the asymptotic validity of the third order expansion (63) appears then to be

$$\varkappa \approx 1 \quad . \tag{90}$$

For a proper stationary solution $I(\Omega)$ to exist in this case, we must have

$$\int L(\Omega')I(\Omega')d\Omega' = [L(\Omega)-\varkappa]/4\varkappa \tag{91}$$

which is impossible even for $\varkappa = 0$. Therefore the stationary solution obtained in the preceeding section for the case $\varkappa = 0$ is not only unphysical on the grounds that one can never have exactly $\varkappa = 0$, but it is also due to an accidental mathematical feature of Eq. (63) which does not belong to the exact Eq. (88).

As an illustration of (88) we have numerically integrated it starting again with a noise level white spectrum, and for several values of the parameter $\varkappa$ (see Fig. 5). For each case we have also plotted the total energy and the spectral width as a function of z. See Figs. 6 and 7.

The most general steady-state solution of Eq. (88) is of the form

$$I(\Omega) = A\delta(\Omega-\Omega_o) \tag{92}$$

where Ω_o is an arbitrary frequency within the passband. Substituting (92) into Eq. (88), one finds that A and Ω_o must be related by

$$\varkappa = L(\Omega_o)/[1 + 4AL(\Omega_o)] \quad . \tag{93}$$

It will now be shown that the solution (92) is stable only if $\Omega_o = 0$. Perturbing the solution (92) by a small amount ϵ, we substitute

$$I(z,\Omega) = A\delta(\Omega-\Omega_o) + \epsilon(z,\Omega) \tag{94}$$

into Eq. (88) and obtain

$$\partial\epsilon(z,\Omega)/\partial z = \{A\delta(\Omega-\Omega_o) + \epsilon\}\{-\varkappa + L(\Omega)\ [1 + 4AL(\Omega_o) + 4\int\epsilon(z,\Omega')L(\Omega')d\Omega']^{-1}\} \ . \tag{95}$$

The correction ϵ occurs in both curly brackets. First order terms are therefore obtained by neglecting ϵ in either one of the two brackets. If the ϵ of the first bracket is neglected, the remaining expression is proportional to $\delta(\Omega-\Omega_o)$ and therefore gives the correction to the δ-function. By neglecting ϵ in the second bracket we can find out about the stability at other frequencies. Equation (95) then reduces to

$$\partial\epsilon/\partial z = \epsilon\{-\varkappa + L(\Omega)\ [1 + 4AL(\Omega_o)]^{-1}\} \quad , \tag{96}$$

and using (93) to

$$\partial\epsilon/\partial z = \epsilon[L(\Omega) - L(\Omega_o)][1 + 4AL(\Omega_o)]^{-1} \tag{97}$$

For the solution (92) to be stable we must therefore have

$$L(\Omega) \leq L(\Omega_o) \text{ for all } \Omega \tag{98}$$

which is only possible if $\Omega_o = 0$.

V. DOPPLER BROADENING

A. Derivation of the Equation

If a group of molecules is moving with velocity v, their resonance frequency is effectively shifted by an amount Kv

$$\omega_{eff} = \omega + Kv \tag{99}$$

where the wave number is defined as

$$K = \omega/c \quad . \tag{100}$$

To lowest order, the partial polarization $P(v,z,t)$ and population inversion $N(v,z,t)$ can be obtained from the corresponding expressions (24b) and (24c) for the case $v = 0$, by simply substituting ω_{eff} for ω. The use of this recipe was justified in the previous work.[33] Carrying out the narrow passband approximation along the lines of Sec. III-3, we find

$$\partial E(z,\Omega)/\partial z = -\varkappa E + \mathcal{G}P(z,\Omega) \tag{101a}$$

$$P(v,z,\Omega) = D(\Omega-Kv)\int N(v,z,\Omega')E(z,\Omega-\Omega')d\Omega' \tag{101b}$$

$$N(v,z,\Omega) = W(v)\delta(\Omega) - F(\Omega)\int d\Omega'[P(v,z,\Omega')E^{*}(z,\Omega'-\Omega) + E(z,\Omega')P^{*}(v,z,\Omega'-\Omega)] \tag{101c}$$

where $\varkappa$, $\mathcal{G}$, $D(\Omega)$, $F(\Omega)$ were defined by (25), (26), (29), (27) respectively and $W(v)$ is the velocity distribution function.

We may build an iterative solution of (101b) and (101c) just as in the case of fixed molecules ($v = 0$). The summation of the polarizations of various orders gives in this case

$$P(v,z,\Omega) = W(v)D(\Omega - Kv)E(z,\Omega)[1 + S(v,z)]^{-1} \tag{102}$$

where

$$S(v,z) = 4\int d\Omega' L(\Omega' - Kv)I(z,\Omega') \quad . \tag{103}$$

The total polarization $P(z,\Omega)$ is obtained by integrating the expression (102) over v. Using the notation

$$\langle \cdots\cdots \rangle_v = \int W(v)\ (\cdots)dv \tag{104}$$

and the scaling of (64), Eq. (101a) yields

$$\partial I(z,\Omega)/\partial z = I(z,\Omega)\{\langle L(\Omega - Kv)[1 + S(z,v)]^{-1}\rangle_v - \varkappa\}. \tag{105}$$

In connection with this equation we shall define the small signal gain profile

$$G(\Omega) = \int dv W(v) L(\Omega - Kv) \quad , \tag{106}$$

the effective gain profile

$$Q(z,\Omega) = \int dv W(v) L(\Omega - Kv)[1 + 4\int L(\Omega' - Kv)I(z,\Omega')d\Omega']^{-1} \tag{107}$$

and their normalized form

$$G'(\Omega) = G(\Omega)/G(0) \tag{108}$$

$$Q'(z,\Omega) = Q(z,\Omega)/G(0) \tag{109}$$

together with the normalized linear loss

$$\varkappa' = \varkappa/G(0) \ . \tag{110}$$

Using the appropriately scaled distance

$$z' = G(0)z \ , \tag{111}$$

we can write Eq. (105) in a compact form as

$$\partial I(z,\Omega)/\partial z' = [Q'(z,\Omega)-\varkappa']I(z,\Omega) \tag{112}$$

B. Two-Velocity Case

The simplest kind of Doppler broadening occurs when the medium consists of two groups of molecules moving with different velocities. One may then assume without loss of generality that the two velocities are of equal magnitude and opposite sign, say $\pm$ u. If there are equal numbers of molecules of each velocity, the gain profile is simply

$$G'(\Omega) = \tfrac{1}{2}[L(\Omega-Ku) + L(\Omega + Ku)]/L(Ku) \tag{113}$$

Figures 8 and 9 illustrate this profile for $Ku = 0.2\ \gamma_{ab}$ and $Ku = \gamma_{ab}$, respectively. The transition between the two shapes occurs at $Ku_R = 0.58\ \gamma_{ab}$. It would therefore be desirable to investigate the two-velocity case for $Ku > Ku_R$ and $Ku < Ku_R$.

1. Numerical Integration

The calculations show that for $Ku = 0.2\ \gamma_{ab}$, a flat input spectrum evolves into a sharp peak around $\Omega = 0$, not unlike the case of homogeneous broadening, while for $Ku = \gamma_{ab}$, the same input evolves into two peaks located at the maxima of the corresponding gain curve. These results are illustrated in Figs. 10 and 11.

For the case $Ku = 0.2\ \gamma_{ab}$ we have integrated the equation starting with an input consisting of two sharp peaks around $\Omega = \pm\ 0.2\ \gamma_{ab}$, and have found a gradual merging of the two peaks into a single one around $\Omega = 0$, as seen in Fig. 12. This result indicates that the eventual outcome depends on the shape of the gain curve rather than on the input. For additional confirmation, we considered the case $Ku = \gamma_{ab}$, but with unequal weights $W(u) = 0.6$ and $W(-u) = 0.4$. The gain profile for this case is shown in Fig. 13. Numerical integration in this case exhibits the formation of a large peak around $\Omega = \gamma_{ab}$ and of a smaller one around $\Omega = \gamma_{ab}$ (see Fig. 14).

2. Steady-State Solutions

We can gain insight into the algebra underlying these numerical results by studying the steady state solutions of Eq. (112). By inspection one can see that these must consist of δ-functions. The simplest such solution is therefore

$$I(\Omega) = A\ \delta(\Omega) \quad . \tag{114}$$

For the two-velocity case, with equal weight, we find that A must satisfy

$$A = (\varkappa'^{-1} - 1)/4L(Ku) \quad . \tag{115}$$

Another possible solution is

$$I(\Omega) = \tfrac{1}{2}A\left[\delta(\Omega - \Omega_o) + \delta(\Omega + \Omega_o)\right] \tag{116}$$

in which case we find

$$A = \left[G'(\Omega_o)/\varkappa' - 1\right]/4G'(\Omega_o)L(Ku) \tag{117}$$

where G' is the gain function of (113). More generally it is possible to find solutions of the form

$$I(\Omega) = A_1\delta(\Omega - \Omega_1) + A_2\delta(\Omega - \Omega_2) \tag{118}$$

but solutions containing more than two δ-functions do not exist. This can be seen by substituting

$$I(\Omega) = \sum_{i=1}^{N} A_i \delta(\Omega - \Omega_i) \tag{119}$$

into Eq. (112) and equating to zero the coefficients of the δ-functions. We find a set of N simultaneous equations

$$G_+ L(\Omega_i - Ku) + G_- L(\Omega_i + Ku) = \varkappa' \quad , \; i = 1,\ldots,N \tag{120}$$

where

$$G_\pm = \left\{2L(Ku)\left[1 + 4\sum_{i=1}^{N} A_i L(\Omega_i \mp Ku)\right]\right\}^{-1} \quad . \tag{121}$$

Equations (120) are incompatible if there are more than two distinct frequencies Ω_i. This result can easily be generalized to the case of n discrete velocities, for which one can find steady-state solutions consisting of up to n δ-functions.

Stability. We shall now investigate the stability of these steady-state solutions. Choosing to work, for simplicity, with the solution (116), we set

$$I(z,\Omega) = I(\Omega) + \epsilon(z,\Omega) \tag{122}$$

and substitute into Eq. (112) to find

$$\partial\epsilon(z,\Omega)/\partial z = \epsilon(z,\Omega)\left\{- \varkappa' + G'(\Omega)\left[1 + 4AL(Ku)G'(\Omega_o)\right]^{-1}\right\} \tag{123}$$

after dropping a term proportional to $\delta(\Omega - \Omega_o) + \delta(\Omega + \Omega_o)$ for the reasons indicated in Sec. IV. 4. Using (117), Eq. (123) can be written as

$$\partial\epsilon/\partial z = \epsilon \left[G'(\Omega) - G'(\Omega_o)\right]\left[1 + 4AL(Ku)G'(\Omega_o)\right]^{-1} . \qquad (124)$$

From Eq. (124) it can be inferred that at points of the Ω axis where $G'(\Omega) > G'(\Omega_o)$, $\epsilon(z,\Omega)$ will grow. Thus for (116) to be a completely stable solution, Ω_o must correspond to an absolute maximum of the gain $G'(\Omega)$.

For the case of the unsymmetrical gain profile of Fig. 13 it can be shown by a similar argument that there exists a stable solution of the form (118). The algebra is more involved and the proof left to Appendix A.

C. Continuum of Velocities

In practice the molecules of the cloud are in thermal motion and have a continuous distribution of velocities which can be assumed to be Maxwellian

$$W(v) = \pi^{-1/2}\, u^{-1} \exp(- v^2/u^2) \quad . \qquad (125)$$

The normalized weak signal gain profile in this case is

$$G'(\Omega) = Z_i\left[(\Omega + i\gamma_{ab})/Ku\right]/Z_i(i\gamma_{ab}/Ku) \qquad (126)$$

where Z_i denotes the imaginary part of the plasma dispersion function

$$Z(\zeta) = \pi^{-1/2} \int_{-\infty}^{+\infty} \exp(-t^2)(t - \zeta)^{-1} dt \tag{127}$$

for

$$\operatorname{Im} \zeta > 0 \quad . \tag{128}$$

Figure 15 illustrates this function for $\gamma_{ab}/Ku = 1$.

1. Doppler Limit ($Ku >> \gamma_{ab}$) .

In this limit Eq. (126) reduces to

$$G'(\Omega) = \exp\left[- \Omega^2/(Ku)^2\right] \quad . \tag{129}$$

A similar limiting form may be obtained for the differential equation (112) itself. Assuming that the spectral density $\bar{I}(z,\Omega)$ varies slowly in a frequency range of the order of γ_{ab}, the saturation integral $S(v,z)$ defined in (103) can be approximated by

$$S(v,z) = 4\int d\Omega' L(\Omega' - Kv) I(z,\Omega') \simeq 4\pi\gamma_{ab} I(z,Kv) \quad , \tag{130}$$

since in the limit $\gamma_{ab}/Ku \rightarrow 0$, the Lorentzian L acts like a δ function. Using the same type of approximation to evaluate the velocity average, we find as the limiting form of Eq. (112)

$$\partial I(z,\Omega)/\partial z = \left\{- \varkappa' + \exp\left[-\Omega^2/(Ku)^2\right]\left[1 + 4\pi\gamma_{ab} I(z,\Omega)\right]^{-1}\right\} I(z,\Omega) \tag{131}$$

This equation can be integrated in closed form and the implicit solution is given by

$$I\left[1 - (I/I_\ell)\right]^{-\varkappa'^{-1}\exp(-\xi^2)} = I(0,\Omega)\left[1 - I(0,\Omega)/I_\ell\right]^{-\varkappa'^{-1}\exp(-\xi^2)}$$
$$\times \exp\left\{\left[\exp(-\xi^2)-\varkappa'\right] z\right\} \tag{132}$$

where

$$\xi = \Omega/Ku \tag{133}$$

and

$$I_\ell(\Omega) = (4\pi\gamma_{ab})^{-1}\left[\varkappa'^{-1}\exp(-\xi^2)-1\right] . \tag{134}$$

It can be seen from (132) that the asymptotic limit of this solution, as $z \rightarrow \infty$, is

$$I(\infty,\Omega) = \begin{cases} I_\ell(\Omega) & \text{if } |\Omega| < \Omega_c \\ 0 & \text{if } |\Omega| \geq \Omega_c \end{cases} \tag{135}$$

where Ω_c defines the half-width of the passband and is given, in the Doppler limit, by

$$\Omega_c = Ku\left[\log(1/\varkappa')\right]^{1/2} \quad . \tag{136}$$

The physical interpretation of the simplified Eq. (131) becomes clear if one compares it to the exact Eq. (112). It is seen from the expression (130) for the saturation term $S(z,v)$, that oscillation at any frequency Ω' saturates the medium for frequencies lying in a small range of the order of γ_{ab} around that frequency Ω'. In the Doppler limit this range is very small compared to the overall width of the spectrum which is of the order of Ku, and the interaction of the various frequency components is neglected, thus leading to the simplified Eq. (131) according to which the frequency components propagate independently of each other. However, it will be seen that this approximation changes the nature of the solutions of the equation. The frequency interaction, although restricted, should not be neglected.

2. Steady-State Solutions

Besides the usual δ-function steady-state solutions, which will be discussed later, Eq. (112) admits a new kind of steady-state solution. Indaed, the bracket on the right-hand side of the equation can be made to vanish identically by a suitable choice of $I(\Omega)$ which would make the velocity average independent of Ω. More precisely we must have

$$\varkappa' = \pi^{-1/2}\left[G(0)\right]^{-1}\int L(\Omega - Kv)\exp(-v^2/u^2)\left[1 + 4\int L(\Omega' - Kv)I(\Omega')d\Omega'\right]^{-1} d(v/u) \tag{137}$$

This equality will hold for every Ω if

$$1 + 4\int L(\Omega' - Kv) I(\Omega') d\Omega' = \pi^{1/2} \eta \left[G(0)\varkappa'\right]^{-1} \exp(-v^2/u^2) \qquad (138)$$

where

$$\eta = \gamma_{ab}/Ku \quad . \qquad (139)$$

The integral equation (138) can be inverted by taking the Fourier transform of both sides of the equation. Using the Fourier transform of the Lorentzian

$$\int_{-\infty}^{+\infty} L(\Omega) e^{-i\Omega t} d\Omega = \pi\gamma_{ab} \exp(-\gamma_{ab}|t|) \qquad (140)$$

and an alternative integral representation of the plasma dispersion function

$$Z(\zeta) = i\int_0^\infty d\mu \, \exp(-\tfrac{1}{4}\mu^2 + i\,\zeta\mu) \quad , \qquad (141)$$

one obtains

$$I(\Omega) = (4\pi\gamma_{ab})^{-1}\left[\varkappa'^{-1} Z_i(\xi + i\eta)/Z_i(i\eta) - 1\right] \qquad (142)$$

In the limit $\eta \to 0$, the plasma function becomes a Gaussian and one recovers the expression (134).

The solution (142), for the spectral density, like (134), becomes negative outside the passband ($|\Omega| \geq \Omega_c$). This is physically unacceptable. However, a truncated form of (142) similar to (135) cannot be used in this case because it would not be a solution of the exact Eq. (112), but only an approximate solution provided $Ku >> \gamma_{ab}$. As a result of this analysis, we can say that in the Doppler limit, the solution of the exact Eq. (112) will behave very much as predicted by its limiting form (131). Namely, it will closely approach the function (135), but once this stage is attained, the approximate equation predicts that the solution will stabilize, whereas according to the exact equation it will not.

In the general case, Eq. (112) admits a sum of any number of δ-functions as steady-state solutions. For the simplest case of a single δ-function, we find an implicit value for the amplitude A, by substituting the expression (114) into Eq. (112).

$$\varkappa' = \pi^{-1/2}\left[G(0)\right]^{-1}\int d(v/u)\exp(-\ v^2/u^2)L(Kv)\left[1 + 4AL(Kv)\right]^{-1} \qquad (143)$$

or in a more convenient form for graphical solution

$$\varkappa'(1 + 4A)^{1/2} = Z_i\left[i\eta(1 + 4A)^{1/2}\right]/Z_i(i\eta) \qquad (144)$$

Solving (144) yields a positive value for A if $0 < \varkappa' < 1$ (as seen in Fig. 16), which in the Doppler limit becomes

$$A = \frac{1}{4}(\kappa'^{-2} - 1) \quad . \tag{145}$$

This δ-function steady-state, which in the case of homogeneous broadening was shown to be stable under all circumstances, will now prove to be stable only under certain conditions. Substituting

$$I(z,\Omega) = A\,\delta(\Omega) + \epsilon(z,\Omega) \tag{146}$$

Into Eq. (112) and dropping as before a term proportional to $\delta(\Omega)$, we find

$$\partial\epsilon/\partial z = \epsilon\Big\{-\kappa' + \pi^{-1/2}\Big[G(0)\Big]^{-1}\int d(v/u)\exp(-\,v^2/u^2)L(\Omega - Kv) \Big[1 + 4AL(Kv)\Big]^{-1}\Big\} \tag{147}$$

Using for κ' its value (143), we can write this result as

$$\partial\epsilon/\partial z = \epsilon\Big\{f(\Omega) - f(0)\Big\} \tag{148}$$

where $f(\Omega)$ is the second term in the curly bracket in (147). It is seen from (148) that for frequencies Ω such that $f(\Omega) > f(0)$, $\epsilon(z,\Omega)$ will grow, hence the solution will be stable only if $f(\Omega)$ has an absolute maximum at $\Omega = 0$. Depending on the values of the parameters Ku and A, $f(\Omega)$ is either a bell-shaped function with an absolute maximum at $\Omega = 0$ or a double-peaked function with a relative minimum at $\Omega = 0$. The first case corresponds to a negative value of the second derivative at $\Omega = 0$ and the second case to a positive value. For the solution to be stable we must therefore have

$$d^2f(0)/d\Omega^2 \leq 0 \quad , \tag{149}$$

or

$$\int d(Kv)\exp(-v^2/u^2)g(A, Kv) \leq 0 \tag{150}$$

with

$$g(A,Kv) = \left[1 + 4AL(Kv)\right]^{-1} d^2L(Kv)/dKv^2 \quad . \tag{151}$$

Setting the right-hand side of (150) equal to zero defines a curve in the (A,Ku) plane which separates the region of stability from the region of instability. The ($\varkappa'$,Ku) plane is similarly devided into two regions since A is a function of $\varkappa'$ and Ku according to (144). The stability condition (150) can be discussed qualitatively in the following way. The function g(A,Kv) is plotted in Fig. 17 for a few values of A. In the extreme Doppler limit ($Ku \to \infty$) the integral of (150) is proportional to

$$\int d(Kv)g(A,Kv) = (\pi/2\gamma_{ab}A^2)\left[1 + A - (1 + 3A)(1 + 4A)^{-1/2}\right] \geq 0 \tag{152}$$

Therefore in this limit the stability condition (150) is never satisfied except for A = 0 which corresponds to $\varkappa' = 1$ (see Fig. 16). It is seen from Fig. 17 and from the condition (150) that for fixed A, the solution will be stable if Ku is smaller than a certain value, depending on A and therefore on $\varkappa'$

$$Ku \leq Ku_{st}(\varkappa') \qquad (153)$$

Inversely, for fixed Ku, the stability condition will be satisfied if A is smaller (consequently $\varkappa'$ larger) than a certain value

$$\varkappa' \geq \varkappa'_{st}(Ku) \quad . \qquad (154)$$

The limiting points are given by

$$\varkappa'_{st}(\infty) = 1 \qquad (155)$$

and

$$Ku_{st}(0) = 1.528\gamma_{ab} \qquad (156)$$

where the last value is given by the root of

$$\int d(Kv)\exp(-\ v^2/u^2)\left[L(Kv)\right]^{-1} d^2L(Kv)/dKv^2 = 0 \qquad (157)$$

which corresponds to (150) with $A = \infty$.

It follows from this discussion that in the $(Ku, \varkappa')$ plane the stability curve has the shape given in Fig. 18

3. Numerical integration

We have integrated Eq. (112) with a digital computer for several choices of the Doppler width Ku and linear loss $\varkappa'$. The cases $Ku = \gamma_{ab}$, $\varkappa' = 0.3$ corresponding to a stable δ-function solution and $Ku = 5\gamma_{ab}$, $\varkappa' = 0.5$ corresponding to an unstable δ-function solution (See Fig. 18) are representative of the two different types of behaviour we found. The first case is illustrated in Fig. 19 which indicates that the solution is approaching a δ-function. Here, the velocity integral involved in Eq. (112) was performed with the use of the Hermite-Gauss integration formula

$$\int_{-\infty}^{+\infty} \exp(-v^2/u^2) Y(v) d(v/u) \simeq \sum_{i=1}^{n} W_i Y(ux_i)$$

where the x_i's are zeros of the nth Hermite polynomial $H_n(x)$ and the W_i's are appropriate weight factors (See ref. 33 Sec. VI. C). For $Ku >> \gamma_{ab}$ this formula cannot be usefully applied and the integration of the equation becomes more time consuming, because the frequency range involved in the integration is of the order of Ku and the integrands are rapidly varying in a range of the order of γ_{ab} which forces one to use a very fine subdivision of the Ω-axis. For this reason, in the physically interesting case in which Ku is very much larger than γ_{ab}, the integration of Eq. (112) becomes prohibitively expensive. We have seen, however, that in this case (132) represents a good approximation to the exact solution, at least over an appreciable distance, but not for $z \to \infty$. In the case of moderately large Doppler broadening ($Ku = 5\gamma_{ab}$) which is shown in Fig. 20, the solution first develops a smooth peak, then becomes irregular and does not evolve into a simple form but shows a more and more granulated structure. This type of behaviour becomes more pronounced if Ku is increased.

VI. CONCLUSIONS

We have seen in Sec. IV that the propagation equations for the electromagnetic field in a two-level amplifier can be reduced to a simple integro-differential equation (112) for the spectral density $I(z,\Omega)$ in the special case of incoherent radiation. The physical content of this equation is that oscillation at any given frequency saturates a range of the order of γ_{ab} around itself

When the passband of the medium is of the order of γ_{ab} as in most of the cases we considered, the whole spectral region of interest comes under the strong saturating influence of oscillation at the central frequency, thus giving an ever-sharpening central peak in the spectral profile. On the other hand, if $Ku \gg \gamma_{ab}$ the region of positive gain is of the order of Ku, provided that $\varkappa'$ is not too close to unity, and the complete spectrum cannot fall under the domination of any single frequency thus leading to a "chaotic" situation. This type of behaviour prevails in the instability region shown in Fig. 18. Notice that no matter how large Ku is, κ' can be chosen so close to unity that the pass-band is effectively reduced to a size such that stability can be favored. It appears that within the framework of our model for maser amplification, the spectral structure of the observed signal is critically dependent on the 'gain thickness' of the amplifying medium, on the ratio of the Doppler width Ku to the natural band-with γ_{ab} and finally on the normalized linear loss κ' which expresses the amount by which threshold is exceeded. Consequently the theory can only yield estimated relationships between these parameters. For example, a spectral width much narrower than the Doppler width Ku requires a considerable thickness but also operation near threshold ($\kappa' \approx 1$), or a natural bandwidth γ_{ab} comparable to Ku. On the other hand if there is reason to believe that the medium is appreciably above threshold and that $\gamma_{ab} << Ku$, then the width of the spectrum gives an estimated lower limit to the kinetic temperature of the medium. However, before drawing any theoretical conclusions of this nature one must be assured, possibly through the use of long base line interferometry, that the observed spectrum is that of a single source rather than a complex superposition of several sources.

APPENDIX A

In this appendix we prove that in the case of two-velocity Doppler broadening with an unsymmetrical gain profile

$$G'(\Omega) = W_1 L(\Omega - Ku_1) + W_2 L(\Omega - Ku_2) \tag{A1}$$

there exists a stable steady-state solution of Eq. (112) of the form

$$I(\Omega) = A_1 \delta(\Omega - \Omega_1) + A_2 \delta(\Omega - \Omega_2) \quad . \tag{A2}$$

Substituting (A2) into Eq. (112) we find that the four unknown quantities A_1, A_2, Ω_1 and Ω_2 must be related by the two following relations

$$\varkappa' = \langle\, L(\Omega_1 - Kv) \left[1 + 4A_1 L(\Omega_1 - Kv) + 4A_2 L(\Omega_2 - Kv)\right]^{-1} \rangle \tag{A3a}$$

$$\varkappa' = \langle\, L\ (\Omega_2 - Kv) \left[1 + 4A\ L(\Omega\ \ - Kv) + 4A_2 L(\Omega_2 - Kv)\right]^{-1} \rangle \quad . \tag{43b}$$

Adding a small perturbation to the solution (A2), we substitute

$$I(z,\Omega) = I(\Omega) + \varepsilon(z,\Omega) \tag{A4}$$

into Eq. (112) and find that the stability at frequencies other than Ω_1 and Ω_2 is governed by the equation

$$\partial\epsilon/\partial z = \epsilon\left\{- \varkappa' + \left\langle L(\Omega - Kv)/\left[1 + 4A_1 L(\Omega_1 - Kv) + 4A_2 L(\Omega_2 - Kv)\right]^{-1} \right\rangle_v\right\} \qquad (A5)$$

which, using (A3) can be written as

$$\partial\epsilon/\partial z = \epsilon\left\{f(\Omega_{1,2}) - f(\Omega)\right\} \qquad (A6)$$

where $f(\Omega)$ is the second term in the curly bracket in (A5) and $\Omega_{1,2}$ stands for either Ω_1 or Ω_2 since

$$f(\Omega_1) = f(\Omega_2) \qquad (A7)$$

according to (A3). The solution will be stable only if Ω_1 and Ω_2 are absolute maxima of $f(\Omega)$. We must therefore have

$$\partial f(\Omega_1)/\partial\Omega = \partial f(\Omega_2)/\partial\Omega = 0. \qquad (A8)$$

The four equations (A3) and (A8) completely determine the parameters A_1, A_2, Ω_1 and Ω_2.

REFERENCES

1. D. R. W. Williams, N. H. Dieter, and H. Weaver, paper presented at the American Astronomical Society Meeting (December, 1965).
2. R. X. McGee, B. J. Robinson, F. F. Gardener, and J. G. Bolton, Nature 208, 1193 (1965).
3. H. Weaver, D. R. W. Williams, N. H. Dieter, and W. T. Lum, Nature 208, 29 (1965).
4. S. Weinreb, M. L. Meeks, J. C. Carter, A. H. Barrett, and A. E. Rogers, Nature 208, 440 (1965).
5. B. Zuckerman, A. E. Lilley, and H. Penfield, Nature 208, 441 (1965).
6. J. L. Yen, B. Zuckerman, P. Palmer, and H. Penfield, Astrophys. J. (Letters) 156, L27 (1968)
7. B. Zuckerman, P. Palmer, H. Penfield, and A. E. Lilley, Astrophys. J. (Letters) 153, L29 (1968).
8. J. A. Ball, and D. H. Stadin, Astrophys. J. (Letters) 153, L41 (1968).
9. M. Sargent, III, and W. E. Lamb, Jr., Phys. Rev. 164, 436 (1967).
10. A. Dienes, Phys. Rev. 174, 400 and 414 (1968).
11. R. A. Settles and C. V. Heer, Appl. Phys. Letters 12, 350 (1968).
12. M. M. Litvak, A. L. McWhorter, M. L. Meeks, and H. J. Z. Zieger, Phys. Rev. Letters 17, 821 (1966).
13. I. S. Shklovsky, Astr. Tsirk. 372 (1966).
14. I. S. Shklovsky, Astr. Tsirk. 424 (1967).
15. M. M. Litvak, ed. Y. Terzian, "Interstellar Ionized Hydrogen" (New York: W. A. Benjamin, Inc.) 1967, 1968. H II Region Symposium, Charlottesville, Va.
16. V. A. Hughes, Nature 215, 942 (1967).

17. P. M. Solomon, Nature 217, 334 (1968).

18. M. M. Litvak, Astrophys. J. 156, 471 (1969).

19. M. M. Litvak, B. Zuckerman, and D. F. Dickenson, Astrophys. J. 156, 875 (1969).

20. J. Z. Holtz, Astrophys. J. (Letters) 153, L117 (1968).

21. B. J. Robinson and R. X McGee, Ann. Rev. Astro. and Astrophys. 5, 183 (1967).

22. A. H. Barrett, Science 157, 881 (1967).

23. W. E. Lamb, Jr., in "Lectures in Theoretical Physics", edited by W. E. Brittin and B. W. Downs, Vol. 2, p. 472 (Interscience Publishers, Inc., New York 1960).

24. L. M. Frantz and J. S. Nodvik, J. Appl. Phys. 34, 2346 (1963).

25. R. Bellman, G. Birnbaum, and W. G. Wagner, J. Appl. Phys. 34, 780 (1963).

26. E. D. Schulz-DuBois, Bell System Techn. J. 43, 625 (1964).

27. J. P. Wittke and P. J. Warter, J. Appl. Phys. 35, 1668 (1964).

28. F. T. Arecchi and R. Bonifacio, J. Quant. Electron. QE-1, 169 (1965)

29. C. L. Tang and B. D. Silverman, in "Physics of Quantum Electronics", edited by P. L. Kelley, B. Lax, and P. E. Tannenwald, (McGraw-Hill Book Co., New York, 1966)

30. N. G. Basov, R. V. Ambartsumyan, V. S. Zuev, P. G. Kryukov, and V. S. Letokhov, Zh. Eksperim. i Teor. Fiz. 50, 23 (1966) [English transl.: Soviet Phys. - JETP 23, 16 (1966)].

31. S. L. McCall and E. L. Hahn, Phys. Rev. Letters 18, 908 (1967).

32. F. A. Hopf and M. O. Scully, Phys. Rev. 179, 399 (1969).

33. A. Icsevgi and W. E. Lamb, Jr., Phys. Rev. 185, 517 (1969).

FIGURE CAPTIONS

Fig. 1. —This figure illustrates the integration of Eq. (43) for 9 discrete frequencies represented by vertical lines whose heights are proportional to the intensities. The phase of each frequency is initially chosen by a random number generator. The linear loss is chosen to be $\varkappa = 0.3\ \mathcal{G}$.

Fig. 2. This figure represents the subdivision of the Ω axis invoked in Eq. (47).

Fig. 3. Lorentzian gain profile.

Fig. 4. Evolution of the spectral density according to Eq. (63) as the radiation propagates through the medium. Curves in order of increasing peak correspond to z = 0, 40, 80, 120, 160 and 200 in units of the reciprocal gain $(2\mathcal{G})^{-1}$. The initially flat spectrum (z = 0) cannot be resolved from the Ω-axis because of the extremely small input value of the intensity (10^{-3}). The linear loss is taken as $\varkappa = 0.3\ \mathcal{G}$.

Fig. 5. The four frames, corresponding to different values of the linear loss $\varkappa$, represent the propagation of the spectrum according to the exact equation (88). In each case, curves in order of increasing peak correspond to $2\mathcal{G}z = 0, 40, 80, 120, 160$ and 200. The first frame may be compared to Fig. 4 which corresponds to the 3rd order Eq. (63).

Fig. 6. The total energy of the radiation is plotted versus the distance, for different values of the linear loss $\varkappa$, according to Eq. (88).

Fig. 7. Plot of the spectral width versus distance for various values of the linear loss parameter, according to Eq. (88).

Fig. 8. Gain profile of Eq. (113) with $Ku = \pm\ 0.2\gamma_{ab}$.

Fig. 9. Two-velocity gain profile as given by Eq. (113), with $Ku = \pm\ \gamma_{ab}$.

Fig. 10. Integration of Eq. (112) for the case of two discrete velocities ($Ku = \pm\ 0.2\gamma_{ab}$), such that the overall gain profile has a single peak as shown in Fig. 8. The spectrum approaches a δ-function at the center of the line. Curves in order of increasing peak correspond to $z' = 0$, 40, 120 and 200. The linear loss is $\kappa' = 0.3$.

Fig. 11. Integration of Eq. (112) for the case of two discrete velocities ($Ku = \pm\ \gamma_{ab}$), such that the overall gain profile has a double peak as shown in Fig. 9. The spectrum evolves, in this case, into two δ-functions. Curves in order of increasing peak height correspond to $z = 0$, 40, 120 and 200. The linear loss is $\kappa' = 0.3$.

Fig. 12. Equation (112) is integrated with a double-peaked input spectrum. The two discrete velocities are $Ku = \pm\ 0.2\gamma_{ab}$ and have equal weights as in Fig. 10.

Fig. 13. Two-velocity gain profile for the case of unequal weights $W(Ku) = 0.6$, $W(-\ Ku) = 0.4$.

Fig. 14. Evolution of the spectrum when the gain is that of Fig. 13. Curves in order of increasing sharpness correspond to $z = 0$, 40 and 80. The linear loss is $\kappa' = 0.3$ and the input value of the spectral density is $I(0,\Omega) = 10^{-2}$, as usual.

Fig. 15. The gain function (126) for the case of a Maxwellian velocity distribution, with $Ku = \gamma_{ab}$.

Fig. 16. Graphical determination of the amplitude A from Eq. (144).

Fig. 17. Plot of the function $g(A,Kv)$ defined in Eq. (151).

Fig. 18. Stability curve in the $(Ku,\varkappa')$ plane. The shaded region corresponds to instability.

Fig. 19. Numerical integration of Eq. (112) with $Ku = \gamma_{ab}$ and $\varkappa' = 0.3$. Curves in order of increasing peak correspond to $z' = 0$, 40, 80, 120, 160 and 200.

Fig. 20. Integration of Eq. (112) with $Ku = 5\gamma_{ab}$ and $\varkappa' = 0.5$. Besides the flat input spectrum lying close to the frequency axis, the spectral profile is shown at $z' = 40$ and $z' = 360$.

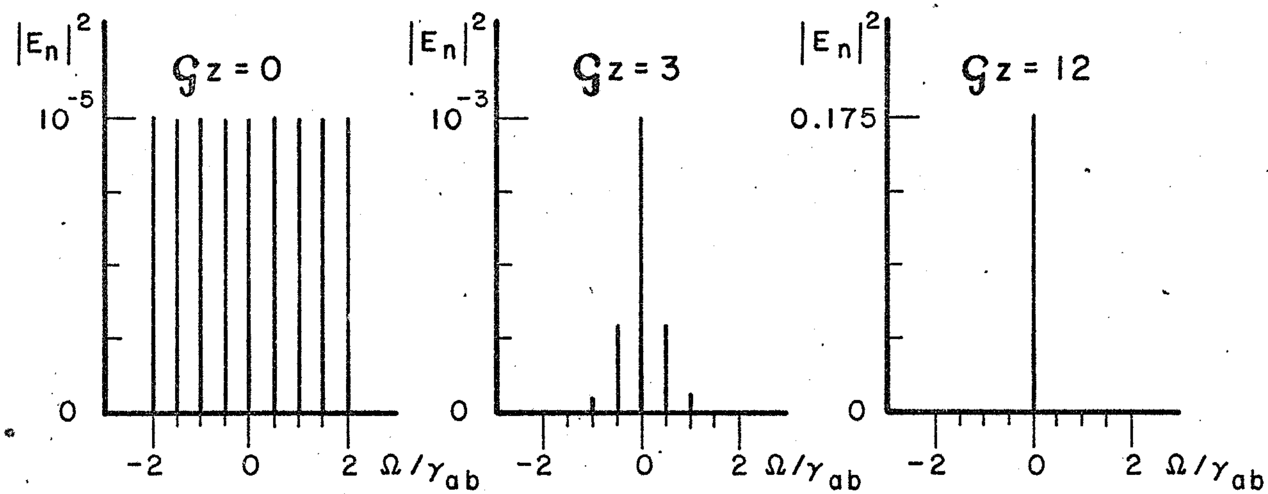

$|E_n|^2$
$\mathcal{G}z = 0$
10^{-5}
0
-2
0
2
Ω/γ_{ab}
$|E_n|^2$
$\mathcal{G}z = 3$
10^{-3}
0
-2
0
2
Ω/γ_{ab}
$|E_n|^2$
$\mathcal{G}z = 12$
0.175
0
-2
0
2
Ω/γ_{ab}

Fig 1

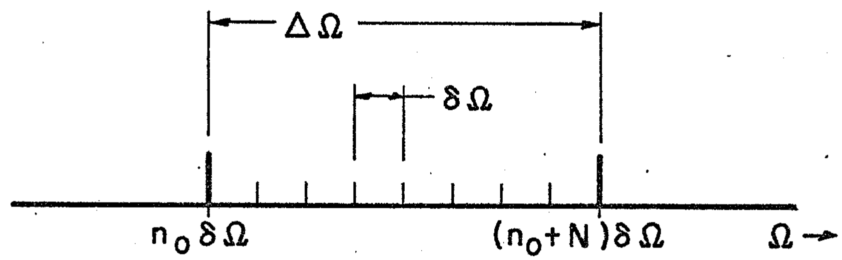

Fig. 2

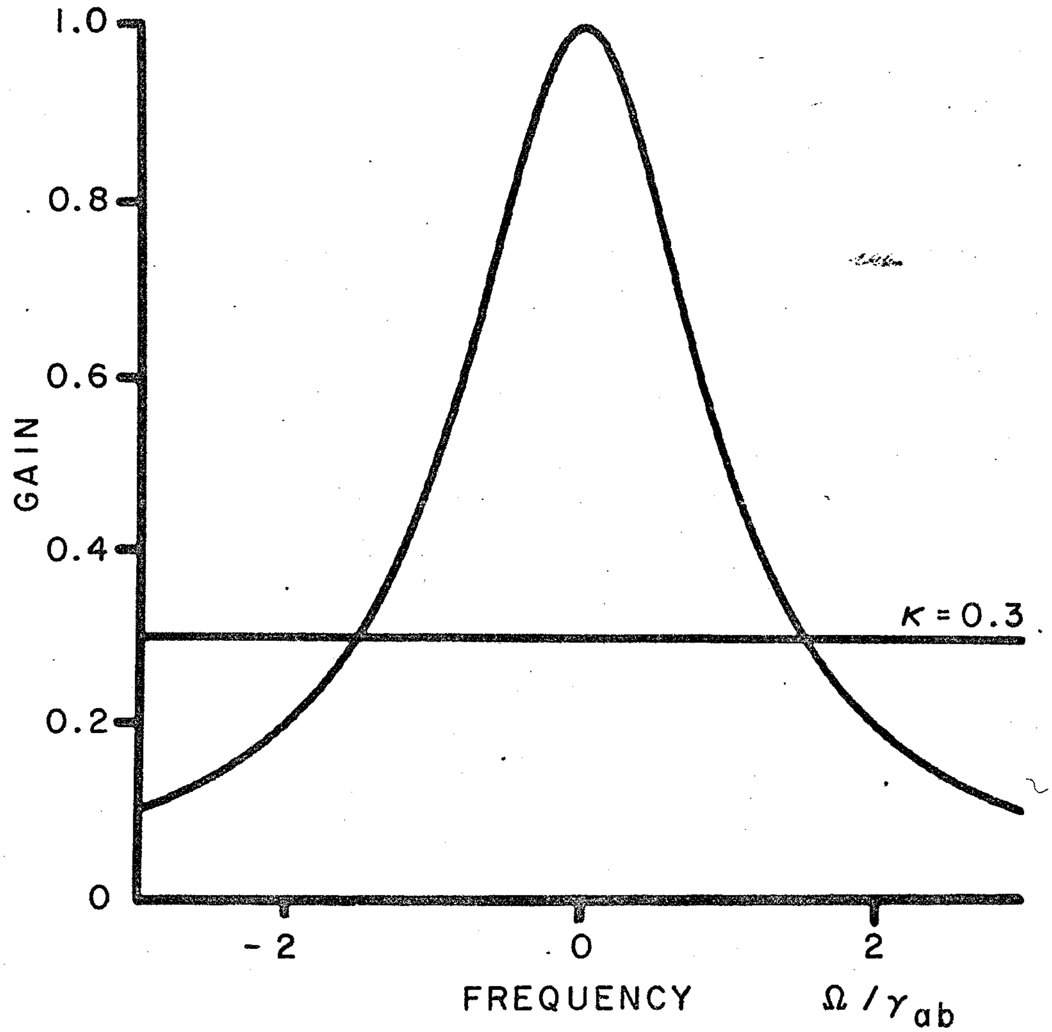

Fig. 3

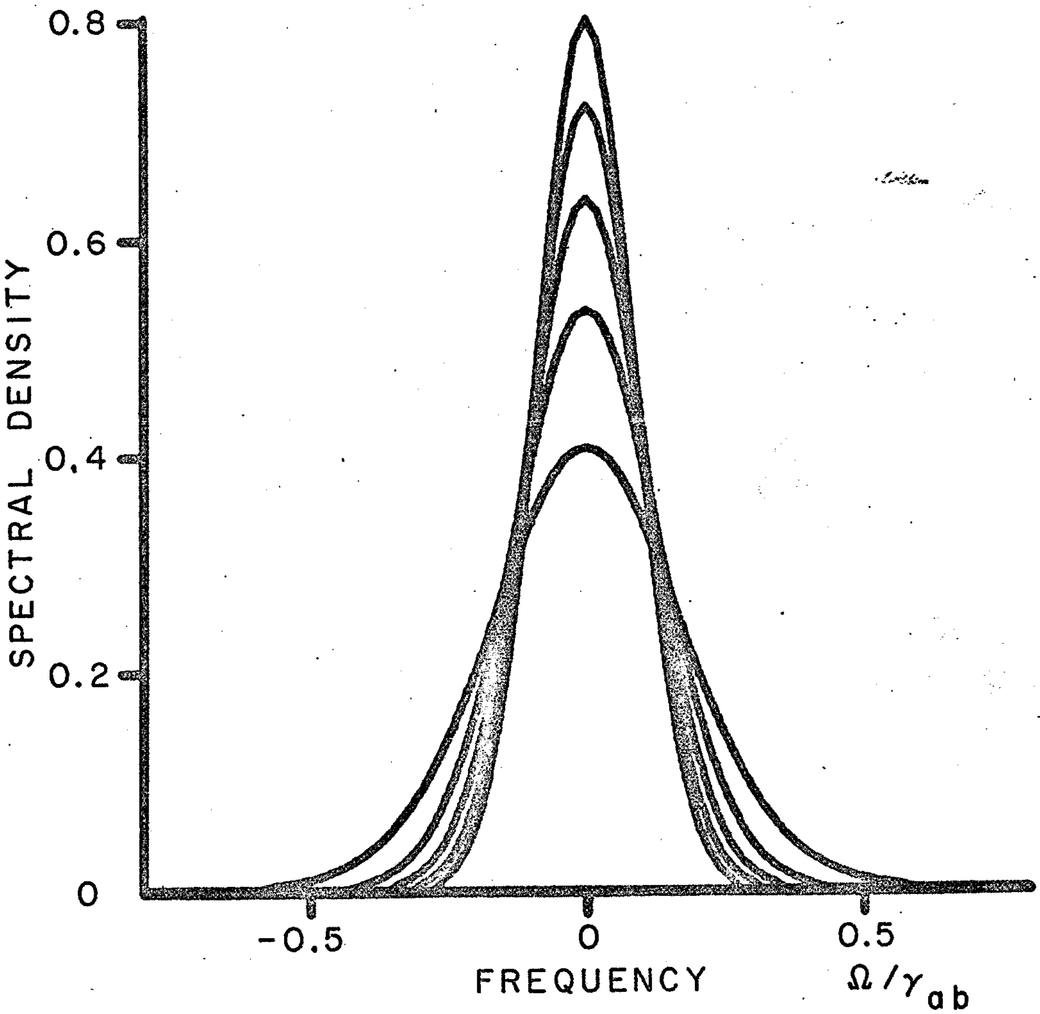

0.8
0.6
0.4
0.2
0
SPECTRAL DENSITY
-0.5
0
0.5
FREQUENCY
Ω/γ_{ab}

Fig 4

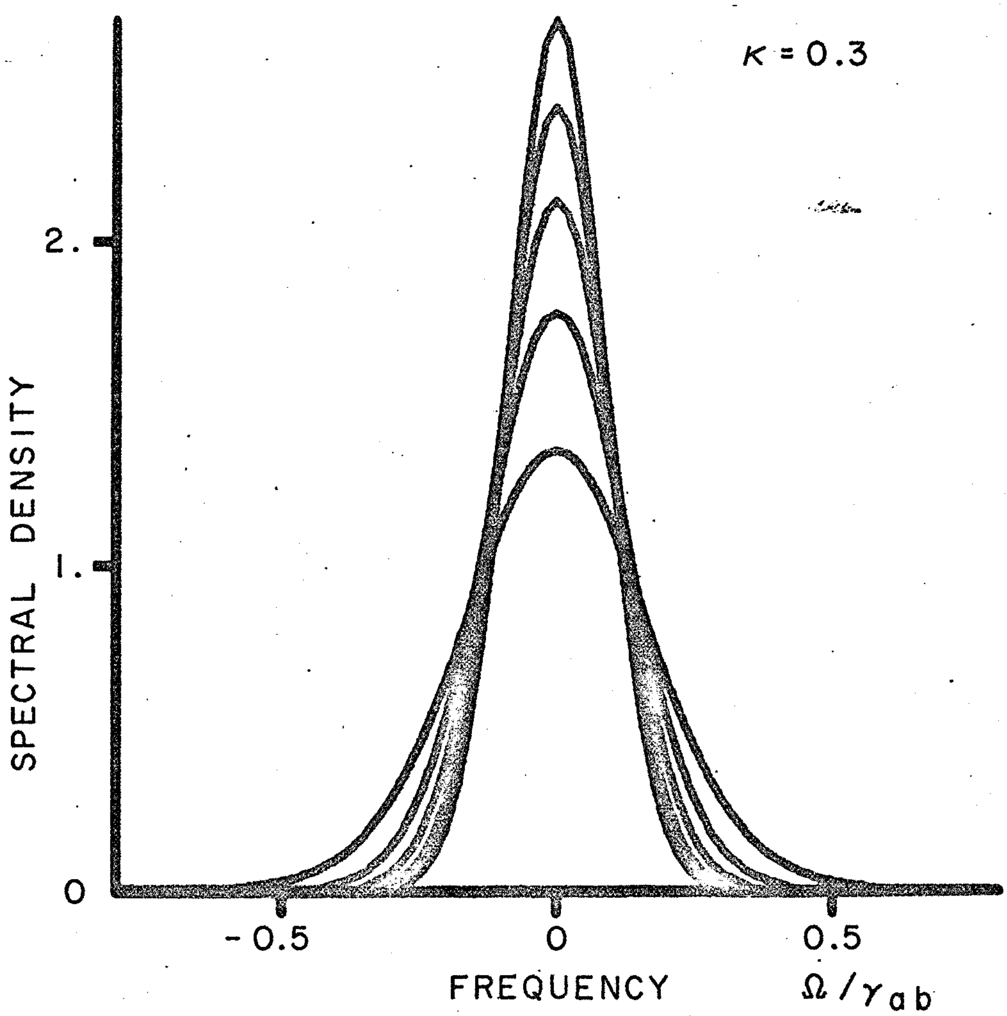

Fig 5a

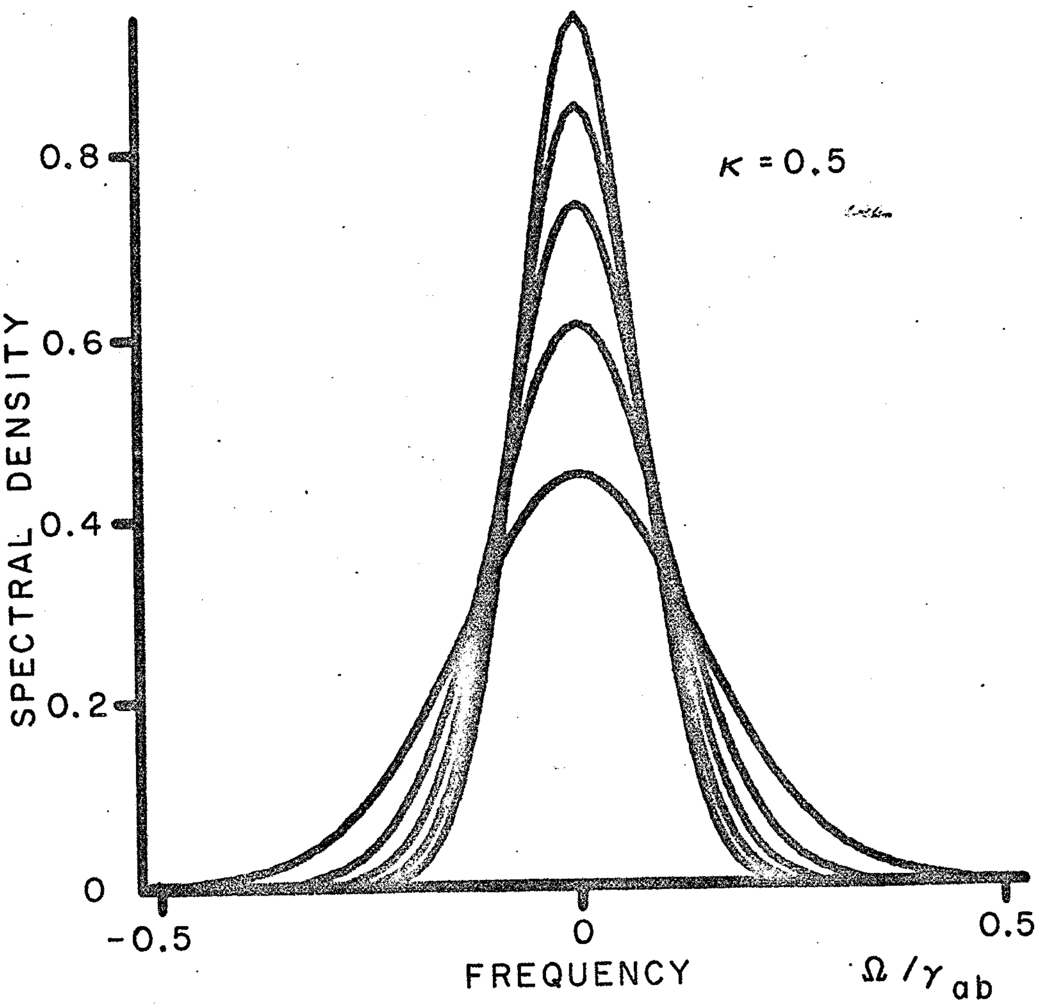

Fig. 5b

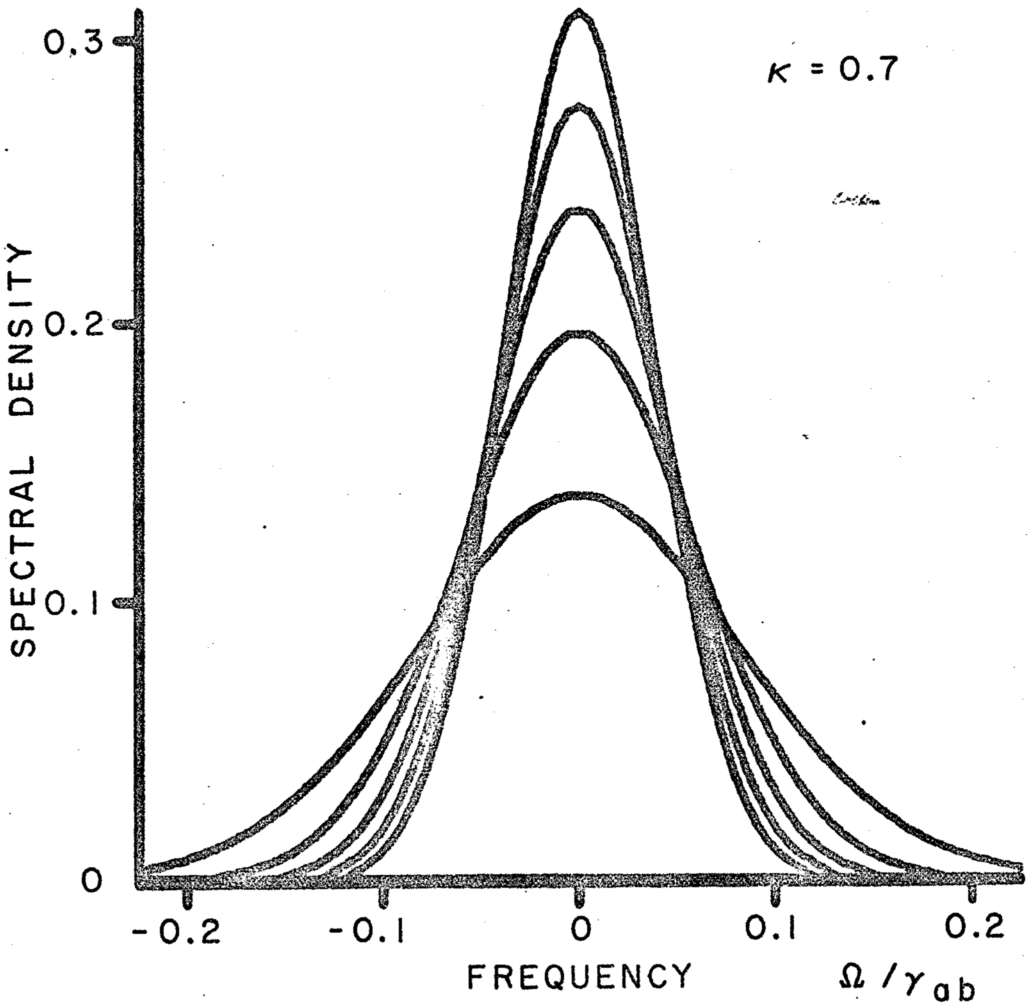

Fig 5c

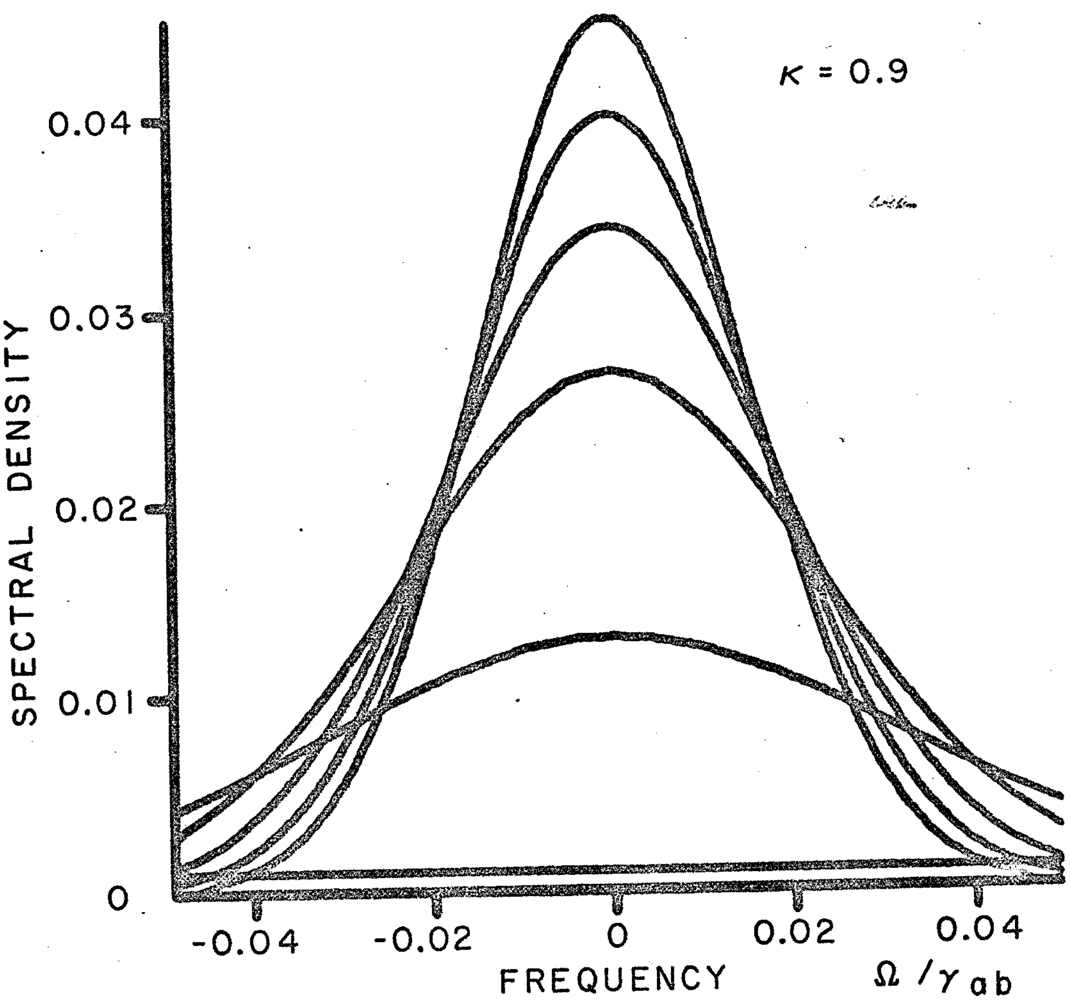
κ = 0.9
SPECTRAL DENSITY
0.04
0.03
0.02
0.01
0
-0.04
-0.02
0
0.02
0.04
FREQUENCY
Ω / γ ab

Fig 5d

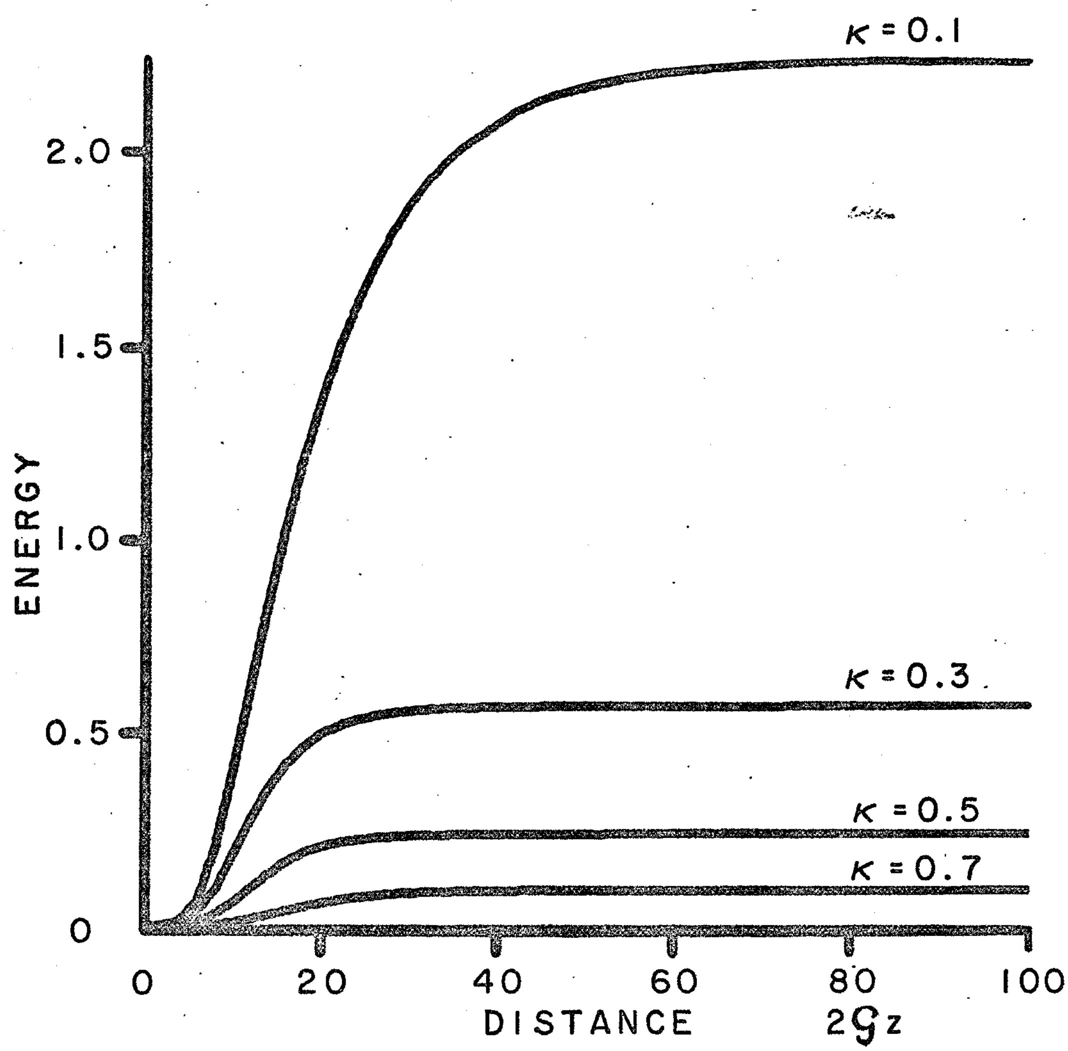

κ = 0.1
κ = 0.3
κ = 0.5
κ = 0.7
ENERGY
2.0
1.5
1.0
0.5
0
0
20
40
60
80
100
DISTANCE 2ϱz

Fig. 6

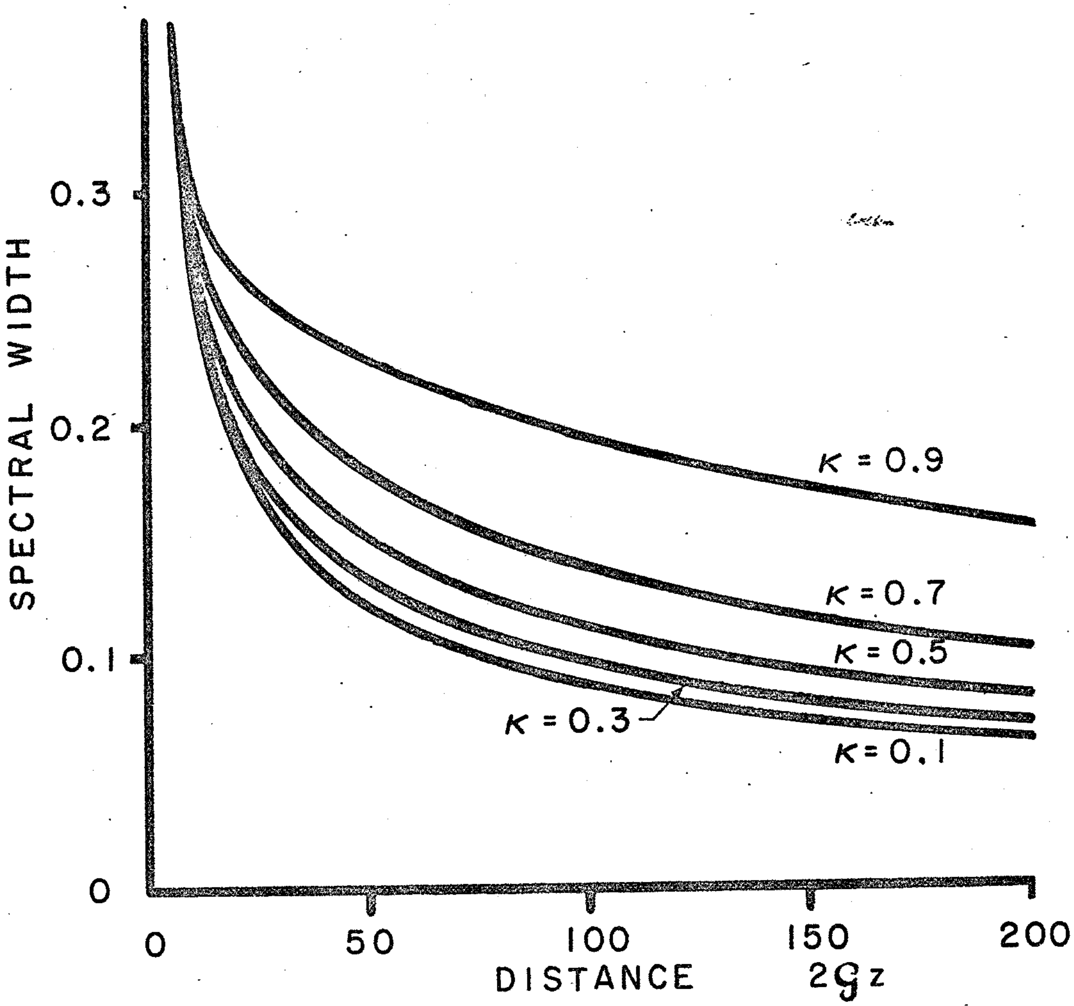

SPECTRAL WIDTH
0.3
0.2
0.1
0
κ = 0.9
κ = 0.7
κ = 0.5
κ = 0.3
κ = 0.1
0
50
100
150
200
DISTANCE 2gz

Fig 7

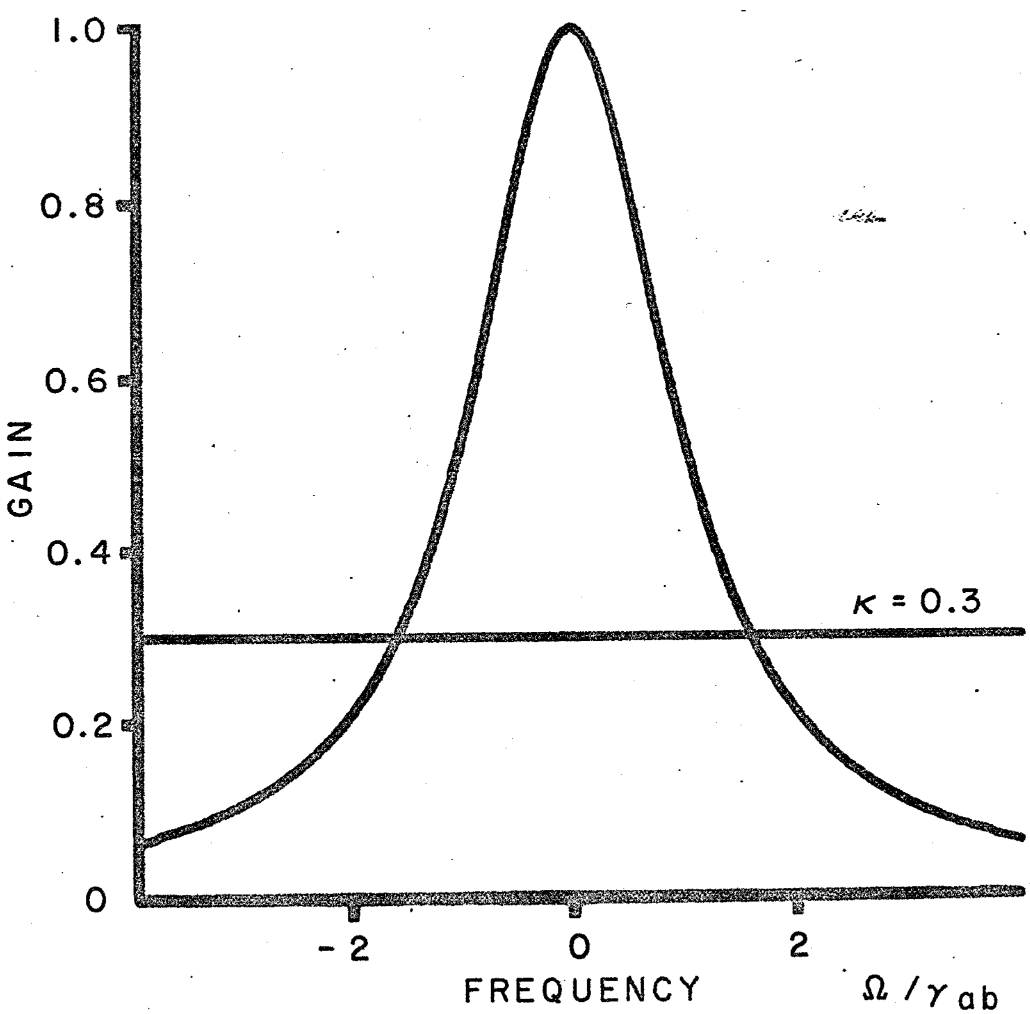

Fig 8

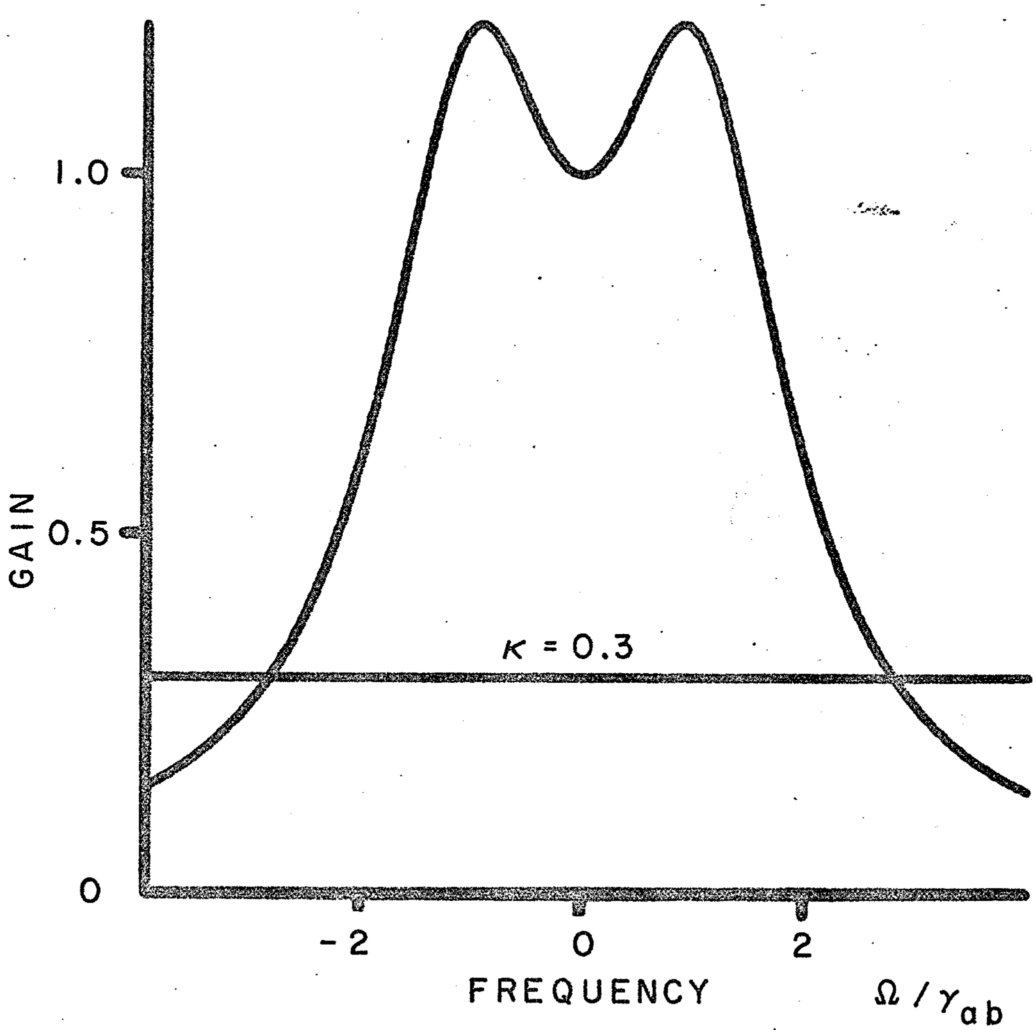

Fig 9

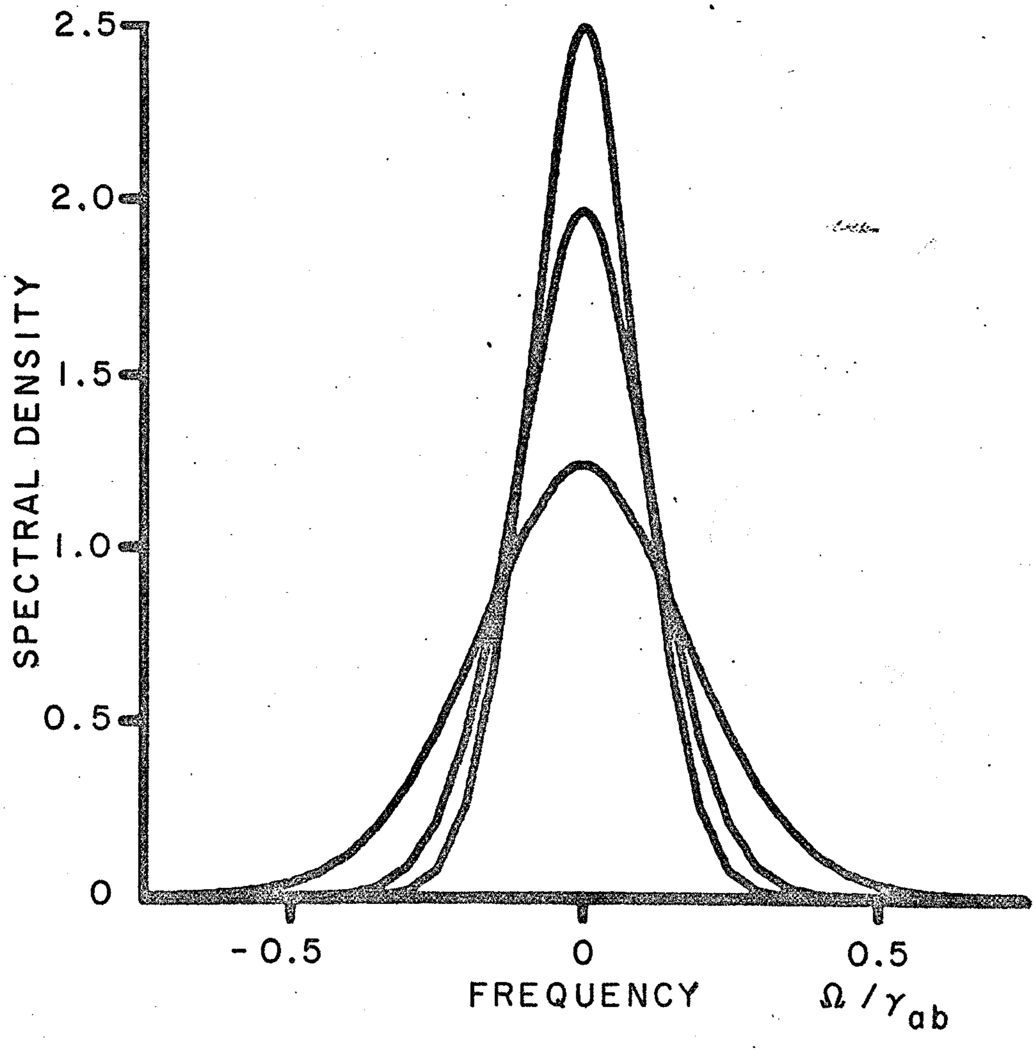

2.5
2.0
1.5
1.0
0.5
0
SPECTRAL DENSITY
-0.5
0
0.5
FREQUENCY
Ω / γ_{ab}

Fig. 10

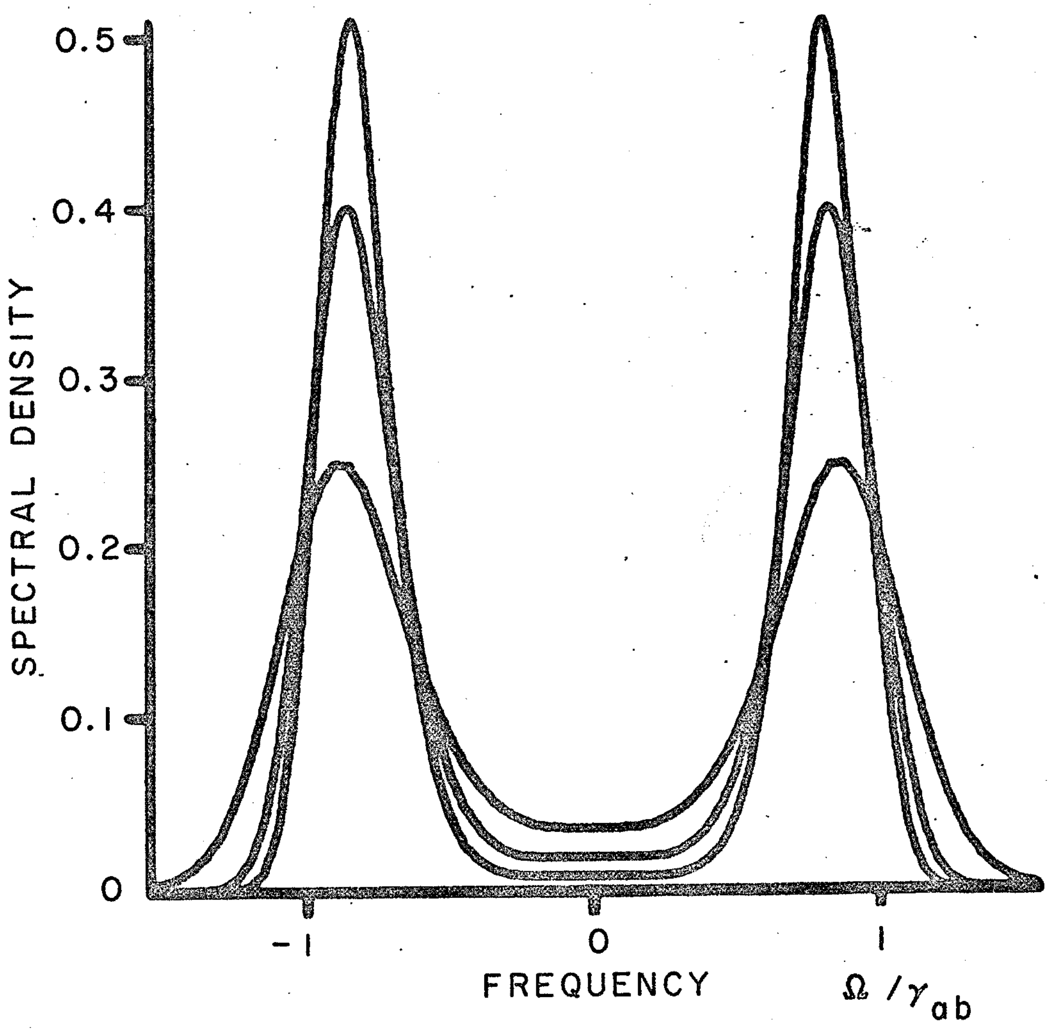

0.5
0.4
0.3
0.2
0.1
0
SPECTRAL DENSITY
-1
0
1
FREQUENCY
Ω / γ_{ab}

Fig. 11

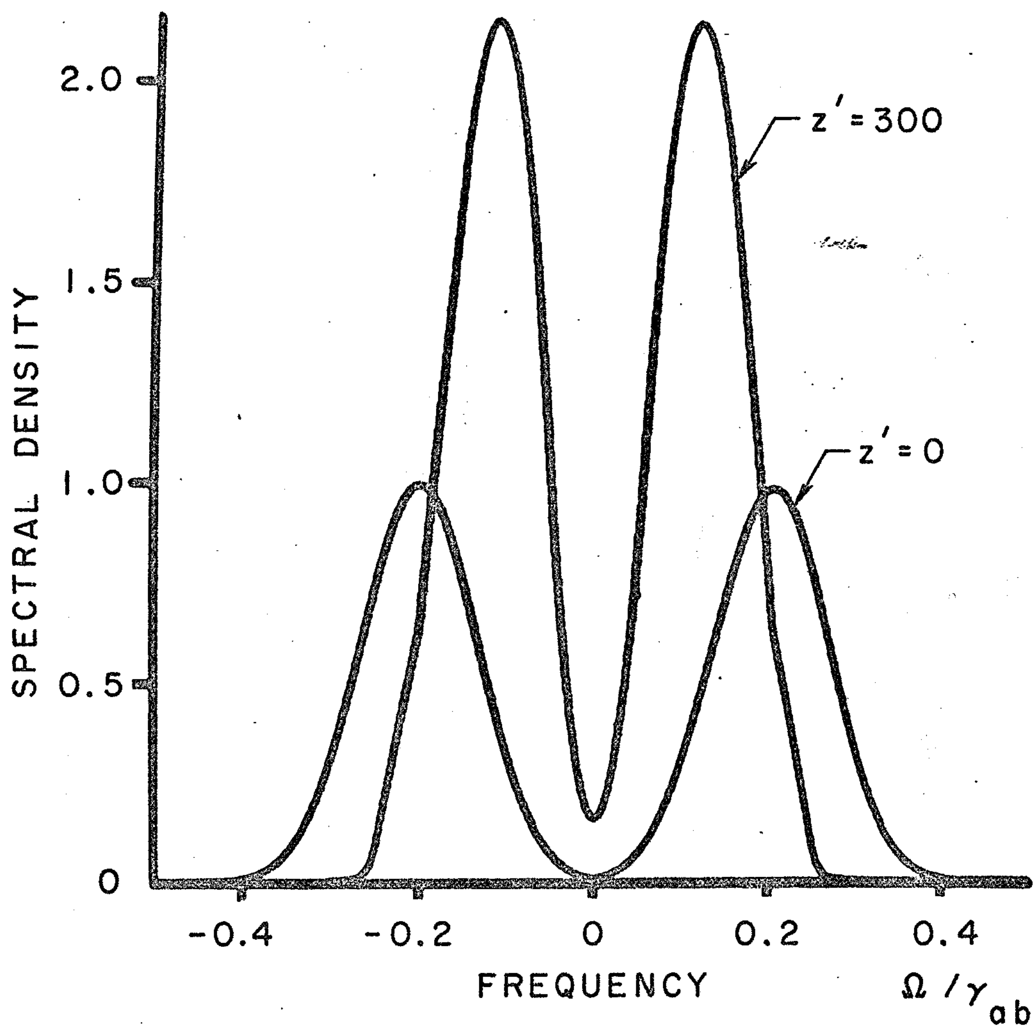
SPECTRAL DENSITY
2.0
1.5
1.0
0.5
0
z' = 300
z' = 0
-0.4
-0.2
0
0.2
0.4
FREQUENCY
Ω / γ_ab

Fig. 12

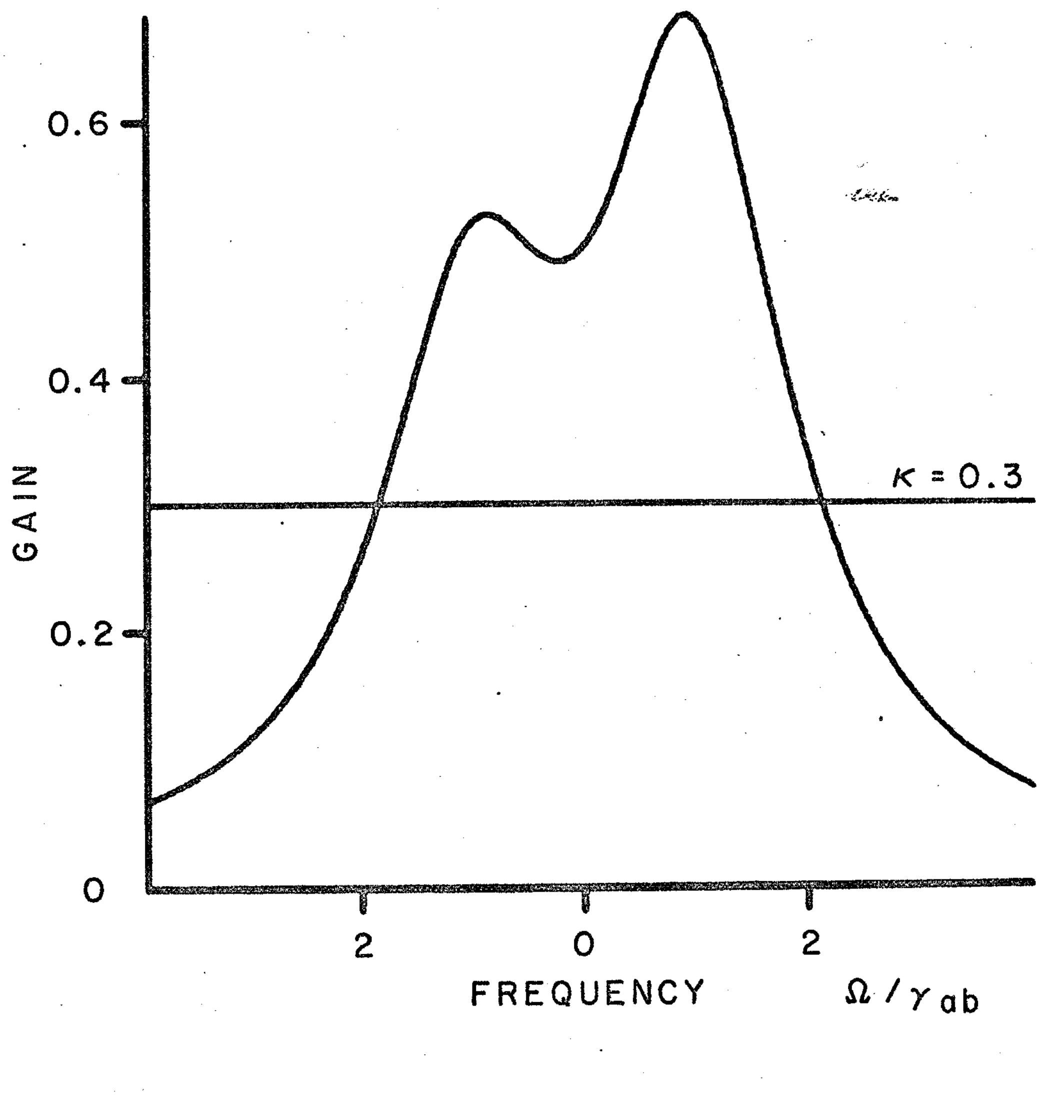

Fig. 13

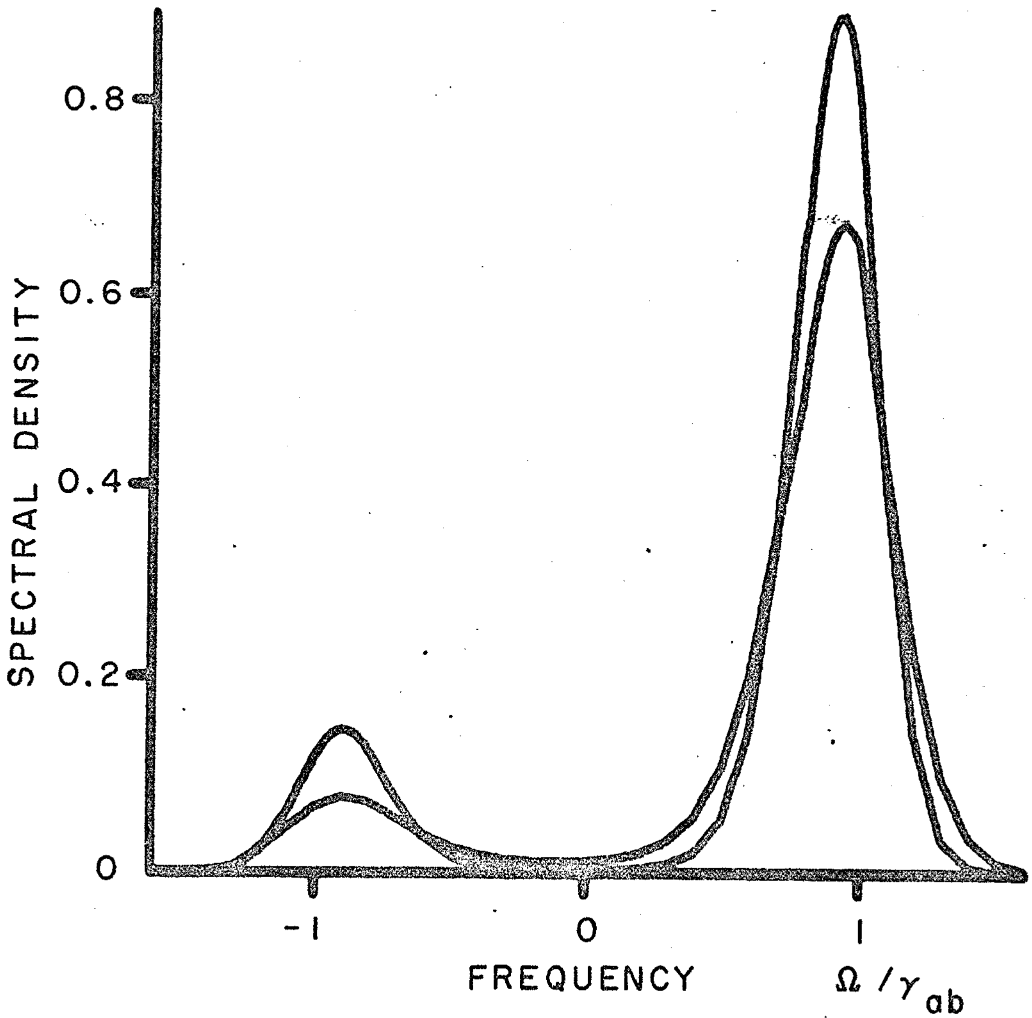

Fig. 1a

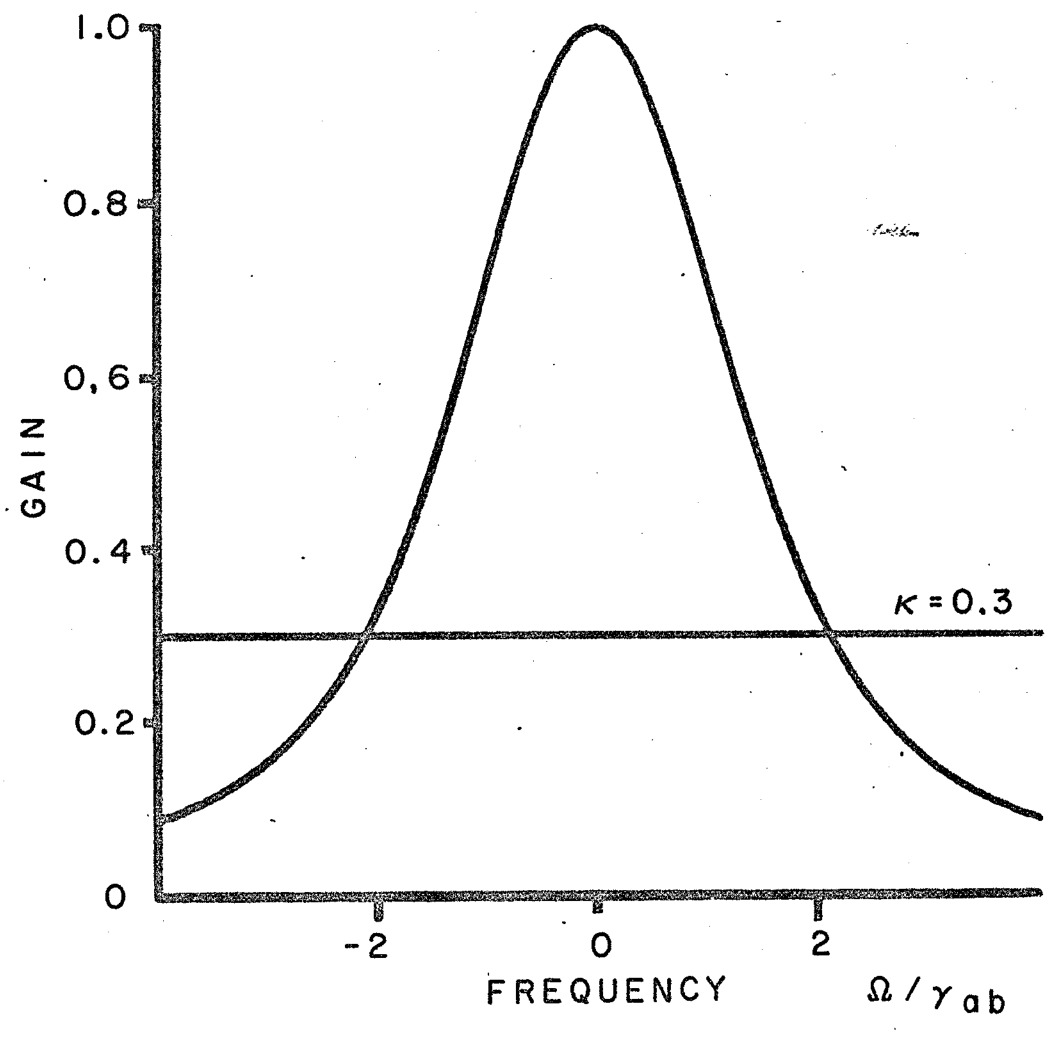

Fig. 15

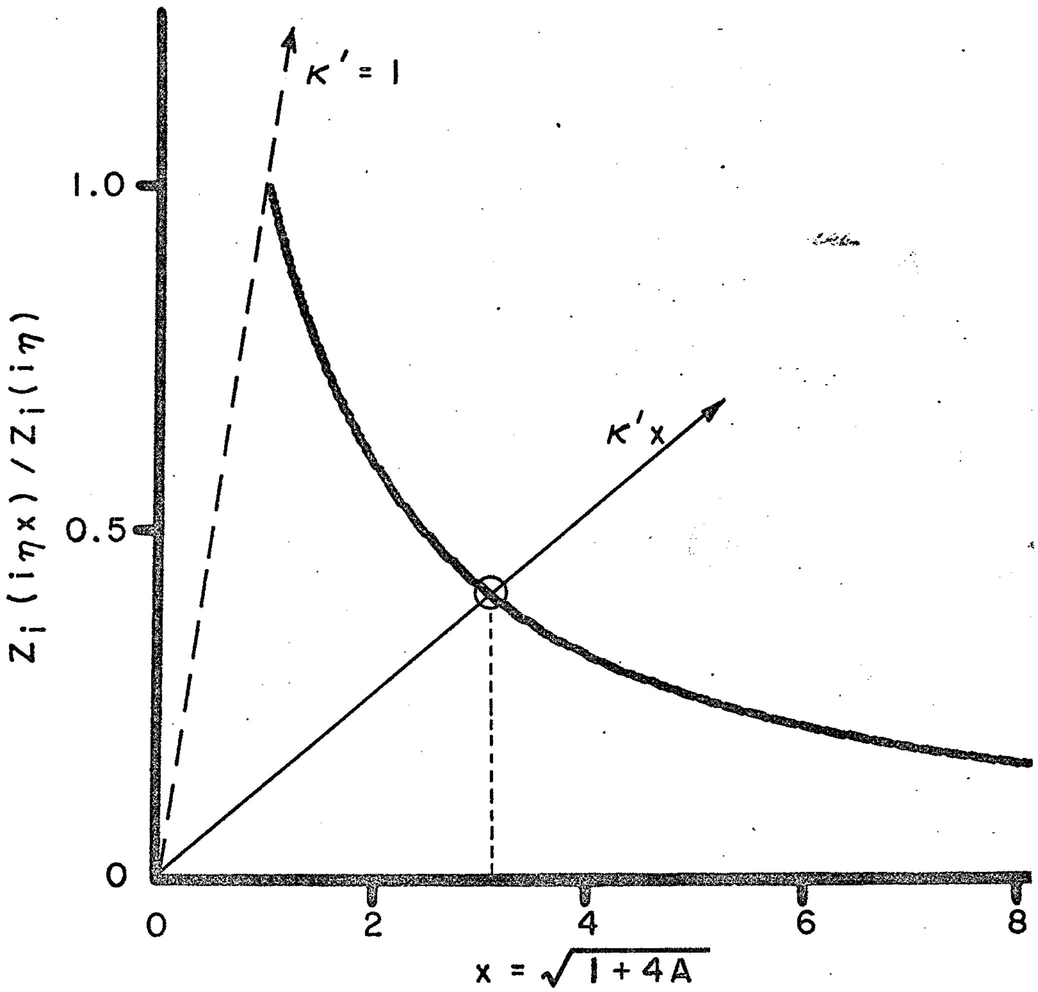

Fig. 16

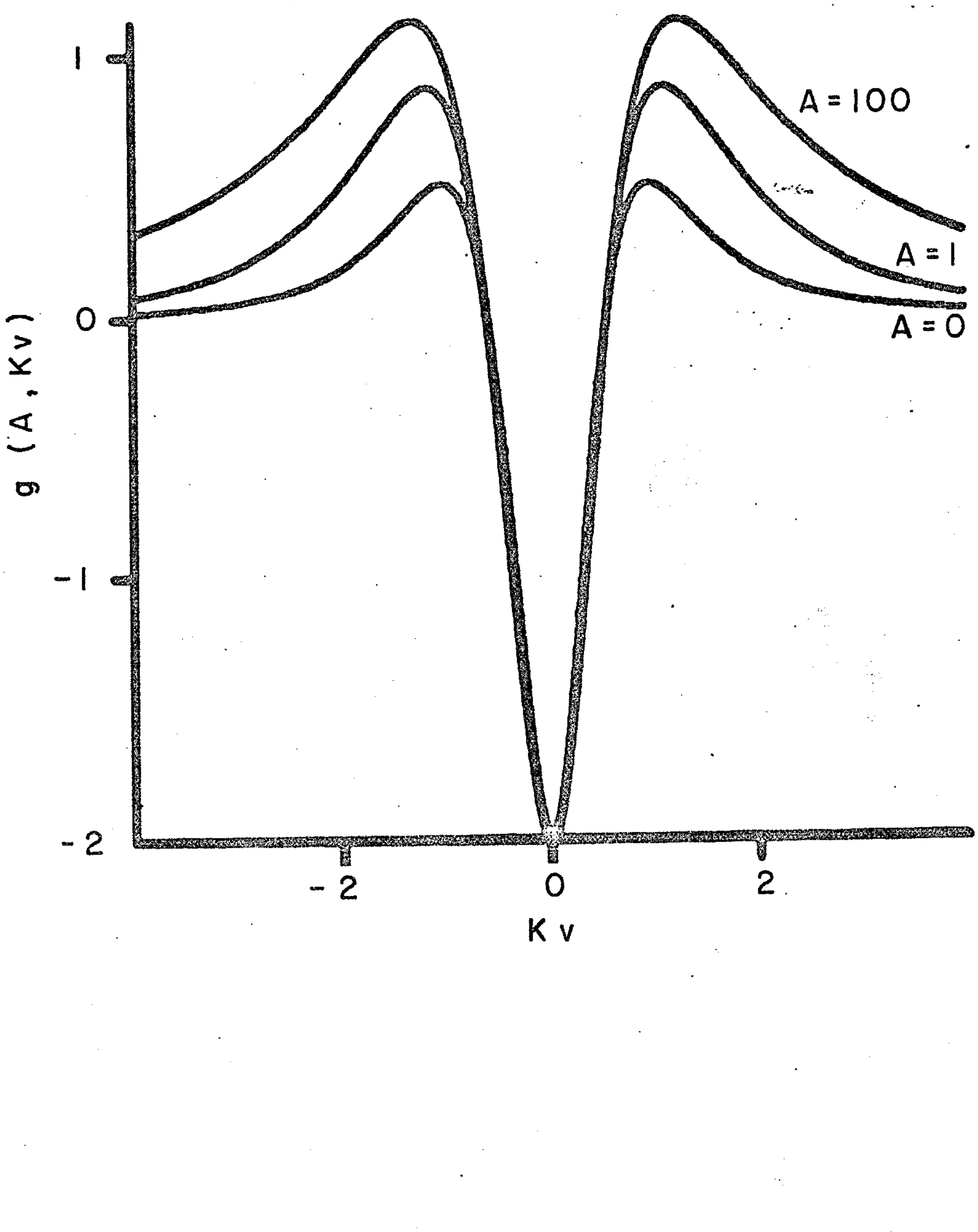

Fig 17

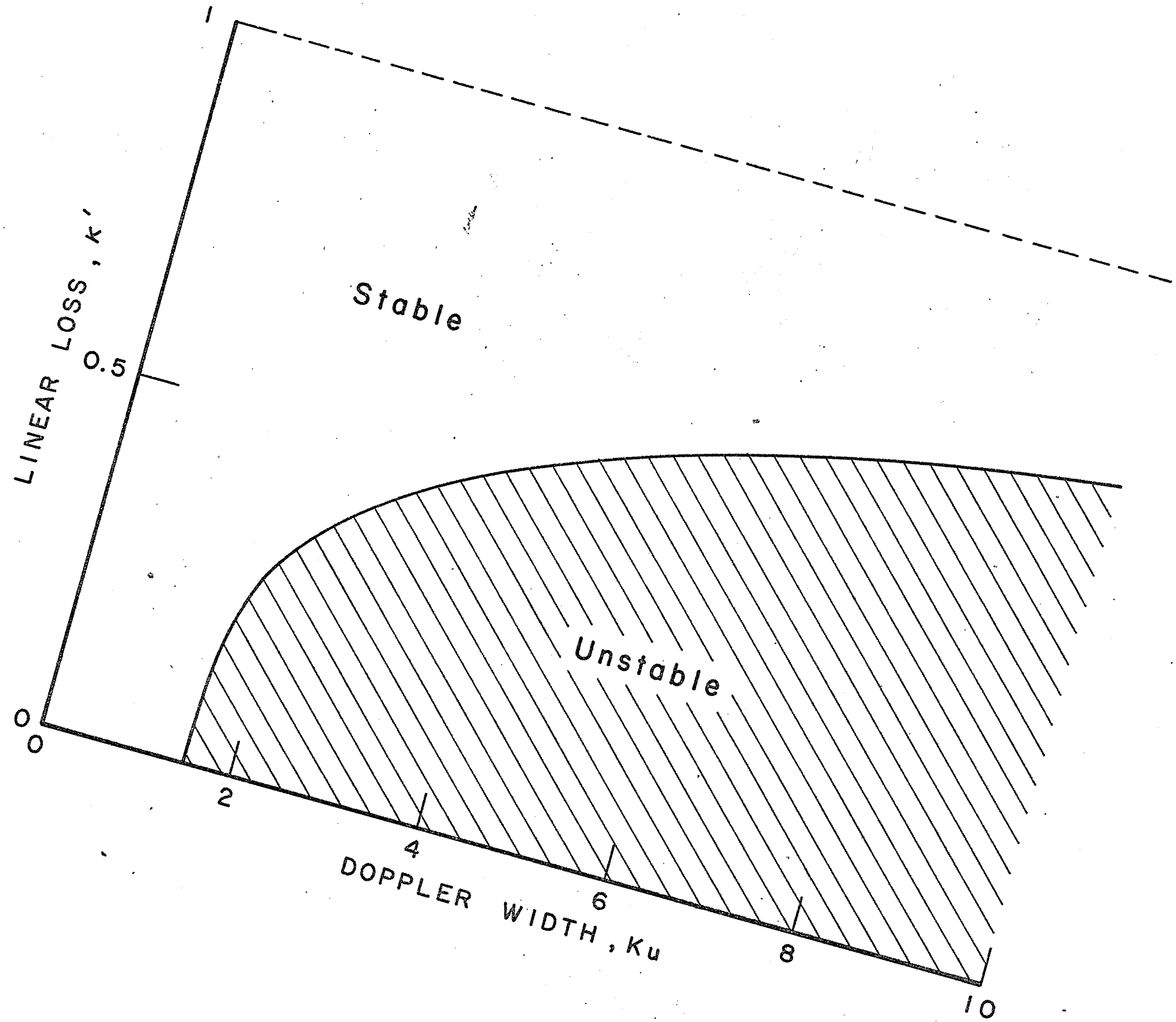
1
0.5
0
LINEAR LOSS, k'
Stable
Unstable
0
2
4
6
8
10
DOPPLER WIDTH, Ku

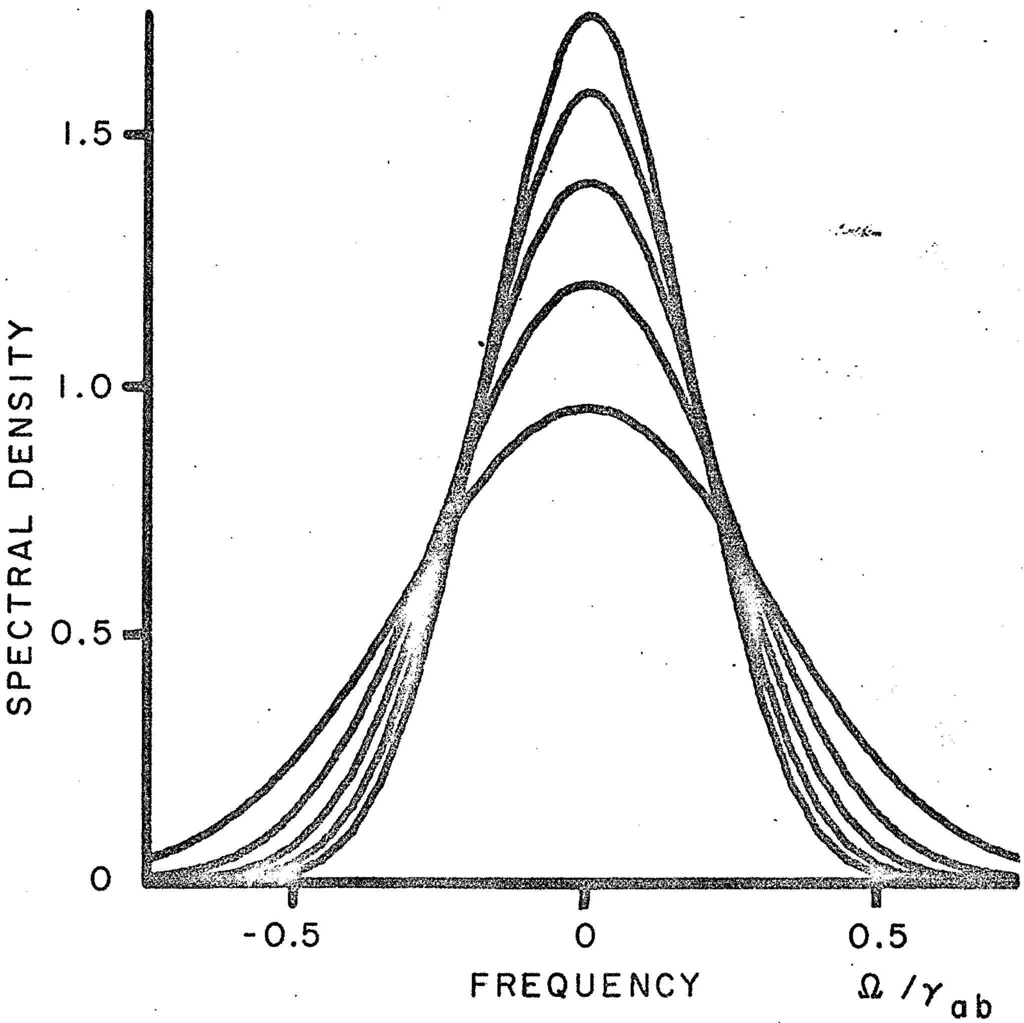

Fig. 19

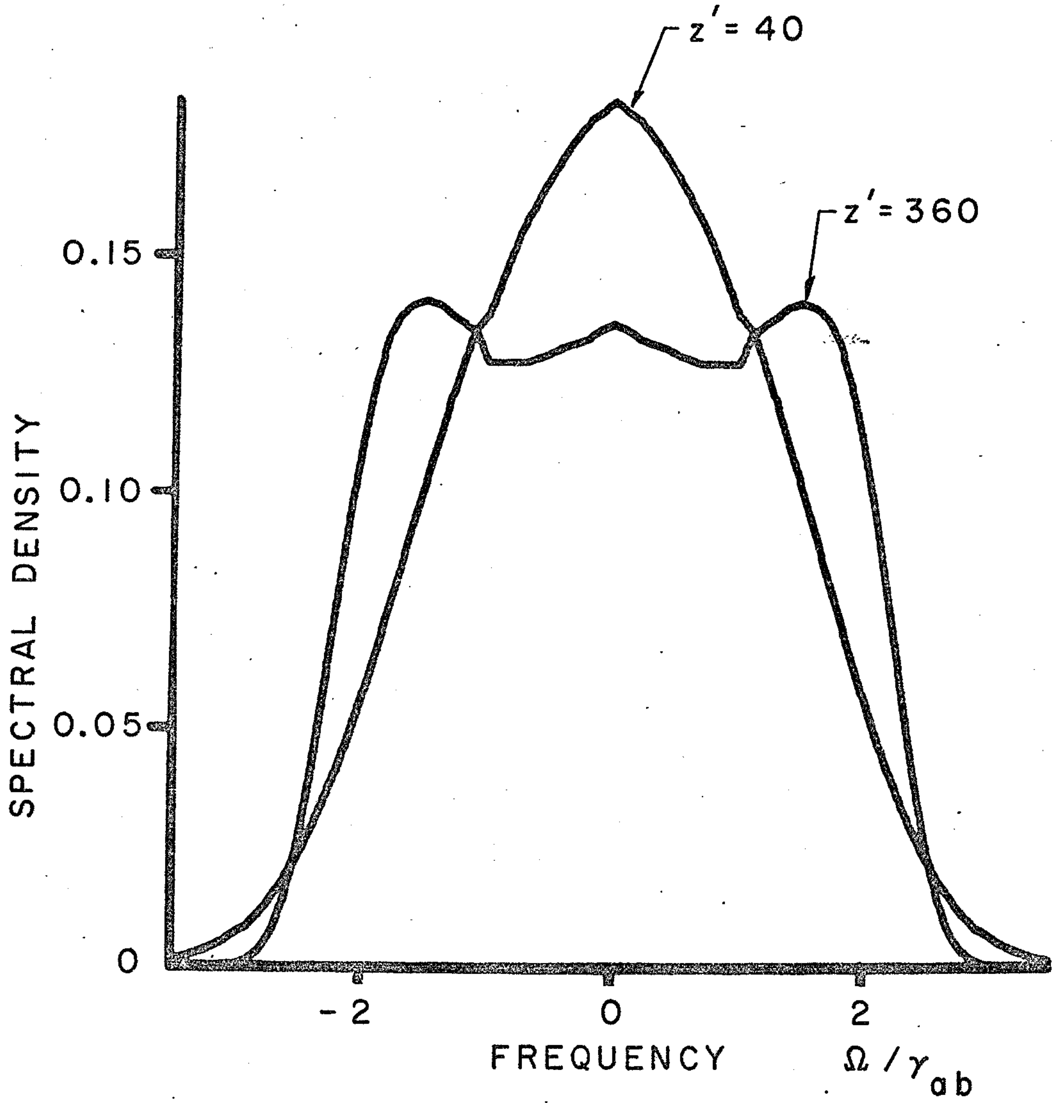

Fig 20